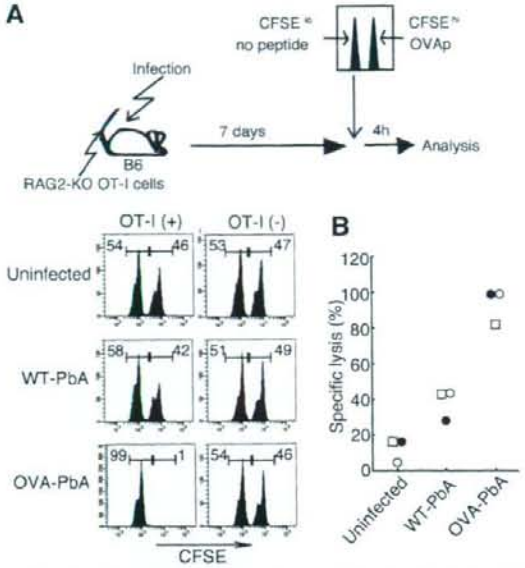

FIGURE 8. Cytotoxicity in vivo of OT-I CD8+ T cells during PbA infection. *A*, B6 mice were uninfected or infected with WT-PbA or OVA-PbA and were inoculated with lymphocytes from RAG2-KO OT-I mice. Seven days later, mice received a 1:1 mixture of differentially CFSE-labeled target splenocytes (1×10^7), and the cytotoxicity was determined 4 h after target cell transfer. Numbers in plots represent the ratio of peptide-pulsed or unpulsed cells. Proportions of OT-I cells in CD8+ T cells: uninfected, 2.7%; WT-PbA, 5.0%; OVA-PbA, 30.7%. Levels of parasitemia: WT-PbA (1.6%) or OVA-PbA (9.7%)-infected B6 mice with OT-I; WT-PbA (8.7%) or OVA-PbA (10.5%)-infected B6 mice without OT-I. *B*, Summary of percent-specific lysis of three similar in vivo cytotoxicity experiments. Result of the experiment in *A* (●) and two other similar experiments using B6 mice transferred with OT-I CD8+ T cells (□, ○) are shown. The variation among experiments was not significant in each group of mice ($p = 0.97$, ANOVA for two-way layout data); hence the data in each group of mice were pooled to compare the difference in percent specific lysis; a significant difference was observed in both overall and paired comparison ($p < 0.05$, ANOVA for one-way layout data).

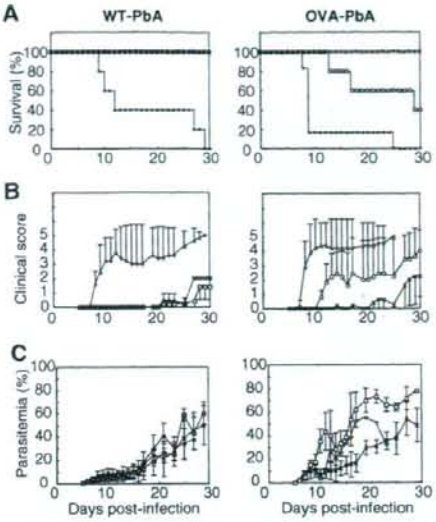

FIGURE 9. Involvement of CD8+ T cell activation in the pathogenesis of PbA. B6 (○), RAG-2 KO (×), and RAG-2 KO OT-I (□) mice were infected with WT-PbA (*left*) or OVA-PbA (*right*). *A*, Kaplan-Meier estimation of survival distributions of mice infected with WT- or OVA-PbA. In WT-PbA-infected mice, survival time in B6 mice was significantly shorter than in other two groups ($p = 0.0018$, log-rank test). In OVA-PbA-infected mice, survival time in B6 mice was significantly shorter than in RAG-2KO OT-I ($p = 0.0165$) and in RAG-2 KO ($p = 0.0014$), whereas the difference in survival time was not significant between RAG-2KO OT-I and RAG-2 KO ($p = 0.0494$). Clinical scores (*B*) and levels of parasitemia (*C*) were also determined in each group after infection. Representative data of two similar results are shown.

To examine whether nonspecific activation occurs in CD8+ T cells expressing other TCR during malaria infection, we used CD8+ T cells from P14-transgenic mice, which express TCR specific for LCMV (26). P14 CD8+ T cells up-regulated CD69, down-regulated CD62L, and expressed granzyme B after infection with WT-PbA, indicating that activation of CD8+ T cells during PbA infection is not limited to OT-I cells (Fig. 6).

CTL function of T cells activated by malaria infection

To determine whether OT-I CD8+ T cells that are activated during PbA infection are able to kill targets, we performed CTL assays in vitro. B6 mice were transferred with OT-I CD8+ T cells and were infected with WT-PbA or OVA-PbA. CD8+ T cells were enriched from these mice and were subjected to ^{51}Cr release assay (Fig. 7*A*). OT-I CD8+ T cells in OVA-PbA-infected B6 mice showed specific CTL activity against OVA-pulsed targets. OT-I CD8+ T cells from WT-PbA-infected mice showed weak but significant OVA-specific killing activity. We also examined CTL activity of CD8+ T cells in RAG2-KO OT-I mice. These cells showed OVA-specific CTL activity after infection with WT-PbA or OVA-PbA, indicating that CTL can be induced without help of CD4+ or other CD8+ T cells (Fig. 7*B*). The CTL activity of OT-I CD8+ T cells from OVA-PbA-infected mice was much higher than those from WT-PbA-infected mice, consistent with their higher expression of granzyme B (Fig. 5*B*).

We also evaluated in vivo killing activity of CD8+ T cells during malaria infection. B6 mice were transferred or not transferred with OT-I CD8+ T cells and were infected with WT-PbA or OVA-PbA. Seven days after the infection, these mice received splenocytes that were differentially labeled with CFSE and were left unpulsed ($CFSE^{low}$) or pulsed ($CFSE^{high}$) with OVAp. The spleen cells were analyzed 4 h later (Fig. 8). OVAp-coated target cells were specifically and almost completely cleared within 4 h in OT-I CD8+ T cell-transferred OVA-PbA-infected mice. Peptide-pulsed targets were also significantly reduced in OT-I CD8+ T cell-transferred WT-PbA-infected mice, although the levels of reduction were much less than those in OVA-PbA-infected mice. These effects were not seen in OT-I CD8+ T cell-transferred uninfected mice or in the infected mice without OT-I CD8+ T cell transfer.

Pathogenesis of CD8+ T cells activated by malaria infection

To determine the role of CD8+ T cells activated during malaria infection, B6, RAG2-KO, and RAG2-KO OT-I mice were infected with WT- or OVA-PbA (Fig. 9). B6 mice died 8–12 days after infection with WT- or OVA-PbA with clinical signs of cerebral malaria. Although the incidence of the cerebral malaria in B6 mice was relatively low (60–80%), it was within the range reported by Amani et al. (35). RAG2-KO mice did not develop cerebral malaria and survived >30 days after infection with WT- or OVA-PbA, consistent with previous studies indicating the requirement for CD8+ T cells in the development of cerebral malaria (7–11).

RAG2-KO OT-I mice were resistant to WT-PbA infection, similar to RAG2-KO mice, and survived >30 days after infection, suggesting that nonspecific activation of $CD8^+$ T cells is not by itself harmful to the host. However, RAG2-KO OT-I mice showed levels of parasitemia higher than RAG-2 KO mice and three of five mice died 13–29 days after infection with OVA-PbA. Although statistical analysis of these data showed that the difference in survival time was not significant between RAG2-KO OT-I and RAG2-KO mice in this particular experiment, we think that it is likely due to the small number of the mice used in this experiment. We observed similar data in another set of experiments; six of seven RAG-2 KO OT-I mice died 15–29 days after infection with OVA-PbA, whereas none of RAG-2 KO mice died within 30 days after infection. Taken together, these data suggest that the activation of malaria-specific $CD8^+$ T cells, in the absence of a diverse adaptive immune system, could lead to the development of lethal pathogenesis during infection with blood stage PbA.

Discussion

This study indicated using a model malaria Ag, OVA, that malaria Ag can be presented to specific $CD8^+$ T cells by APCs in TAP-dependent cross-presentation during infection with PbA. The requirement of TAP for this pathway suggests that cross-presentation of malaria Ags involves the phagosome-to-cytosol pathway, in which Ags are exported to the cytosol after engulfment and are transported into the ER via TAP molecules, as reported for some other microorganisms such as *M. tuberculosis* and *T. gondii* (12, 13, 18, 19). Although infection with the malaria parasite might modulate the function of DCs or inhibit cross-presentation (30, 36–38), our study clearly indicates that APCs are able to cross-present malaria Ags that they have engulfed and activate specific $CD8^+$ T cells during the erythrocyte stage of malaria infection. Although we used a model Ag, OVA, it is likely that the endogenous malaria Ags are presented in a similar manner. The identification of natural CTL epitopes expressed in the erythrocyte stage of malaria parasites would aid our understanding of the role of $CD8^+$ T cells against the malaria blood stage.

In addition to Ag-specific response of $CD8^+$ T cells, we have found that Ag-nonspecific $CD8^+$ T cells could proliferate, show activation phenotype, express granzyme B, and gain CTL function when the host mice were infected with PbA, albeit at a lower level. A couple of possibilities might account for this nonspecific activation of OT-I $CD8^+$ T cells. First, OT-I $CD8^+$ T cells might directly recognize the PbA epitope by cross-reactivity of their TCR. We think that this possibility is unlikely, because OT-1 $CD8^+$ T cells were activated not only in B6, but also in TAP-KO hosts, which are defective in the phagosome-to-cytosol pathway of Ag presentation, suggesting that the activation of OT-I $CD8^+$ T cells in vivo by WT-PbA did not require TCR engagement. In addition, a similar activation-phenotype was observed in $CD8^+$ T cells of P14 TCR-transgenic mice as well as other RAG2-KO TCR-transgenic mice during infection with malaria parasites (Fig. 6 and unpublished observations). Second, host $CD8^+$ T cells might be activated by parasite products via interaction with their receptors other than TCR. Naive and activated $CD8^+$ T cells express a variety of pathogen-recognizing receptors including TLRs (39). Engagement of these receptors with ligands derived from parasites might modulate T cell function without TCR signaling. In particular, it is known that TLR2 is expressed on activated T cells and exhibits costimulatory function for TCR-stimulated T cells or can directly induce Th1 effector function (40, 41). Malaria parasites express GPI anchors that are recognized by TLR2 (42), thus possibly directly modulating the function of host T cells. However, the activation of naive $CD8^+$ T cells by TLR stimulation has not been reported. A third possibility is that $CD8^+$ T cells are activated by cytokine(s) produced by the innate immune system in response to PbA infection (43–45). Our study suggested that NK cells are involved in nonspecific activation of $CD8^+$ T cells. NK cells produce cytokines such as IFN-γ and TNF-α during malaria infection (31). Naive T cells can be activated by cytokines without TCR engagement, which has been termed the innate T cell activation pathway (46). Taken together, it is likely that cytokines produced by NK cells, in combination with products of malaria parasites, participate in Ag-nonspecific activation of $CD8^+$ T cells during infection with PbA.

We demonstrated that two types of $CD8^+$ T cells are activated during malaria infection: those specific for malaria Ag and activated by TAP-dependent Ag presentation; and those activated nonspecifically. In both types of activation, $CD8^+$ T cells express the activation phenotype and granzyme B and can develop into functional CTL, although the levels of the nonspecific activation are much lower than the specific activation. Our study suggested that $CD8^+$ T cells that are activated in an Ag-specific manner are involved in the pathogenesis of severe malaria. Highly activated OT-I $CD8^+$ T cells preferentially sequestered in the brain of B6 mice that were transferred with OT-I cells and infected with OVA-PbA (Fig. 3). In this experiment, however, it was unclear whether these cells were involved in the pathogenesis of cerebral malaria, since host B6 $CD8^+$ T cells were sufficient to cause cerebral malaria. In contrast, RAG2-KO OT-I mice that were infected with OVA-PbA showed early death when compared with RAG2-KO mice, suggesting that activation of OT-I $CD8^+$ T cells was pathogenic to the host, likely due to bystander mechanisms (Fig. 9). OVA-PbA-infected RAG2-KO OT-I mice showed more severe parasitemia and died later than B6 mice, suggesting that the death of RAG2-KO mice was not caused by cerebral malaria but may have been caused by other pathological processes associated with the infection. Taken together, these results suggest that the activation of malaria-specific $CD8^+$ T cells can be pathogenic to the host, but the development of cerebral malaria may require additional factors as has been discussed (10, 11). On the other hand, RAG2-KO OT-I mice showed a clinical course indistinguishable from RAG2-KO mice when infected with WT-PbA, suggesting that $CD8^+$ T cells that are activated in an Ag-nonspecific manner are generally not pathogenic to the host. Nonspecific activation of $CD8^+$ T cells, however, does not require TCR engagement and thus might include a pool of peripheral $CD8^+$ T cells that recognize various MHC class I-bound epitopes including self-Ag. Therefore, it remains possible that activation and CTL development of the self-reactive pool of peripheral $CD8^+$ T cells could lead to the destruction of tissue and might be involved in the pathogenesis of malaria. Further studies on the molecular mechanisms underlying the malaria-specific and nonspecific activation of $CD8^+$ T cells are important for expanding our understanding of protection against *Plasmodium* infection and of the pathogenesis of severe malaria.

Acknowledgments

We thank Drs. H. Kosaka, W. R. Heath, Y. Takahama, and Y. Yoshikai for providing mice; M. Ueda, T. Ikeda, and K. Kimura for technical assistance; Y. Akiyama for help; and Dr. K. Suzue for discussion.

Disclosures

The authors have no financial conflict of interest.

References

1. Suss, G., K. Eichmann, E. Kury, A. Linke, and J. Langhorne. 1988. Roles of CD4- and CD8-bearing T lymphocytes in the immune response to the erythrocytic stages of *Plasmodium chabaudi*. *Infect. Immun.* 56: 3081–3088.

2. Kumar, S., M. F. Good, F. Dontfraid, J. M. Vinetz, and L. H. Miller. 1989. Interdependence of CD4$^+$ T cells and malarial spleen in immunity to *Plasmodium vinckei vinckei*: relevance to vaccine development. *J. Immunol.* 143: 2017–2023.
3. Pombo, D. J., G. Lawrence, C. Hirunpetcharat, C. Rzepczyk, M. Bryden, N. Cloonan, K. Anderson, Y. Mahakunkijcharoen, L. B. Martin, D. Wilson, et al. 2002. Immunity to malaria after administration of ultra-low doses of red cells infected with *Plasmodium falciparum*. *Lancet* 360: 610–617.
4. Good, M. F., H. Xu, M. Wykes, and C. R. Engwerda. 2005. Development and regulation of cell-mediated immune responses to the blood stages of malaria: implications for vaccine research. *Annu. Rev. Immunol.* 23: 69–99.
5. Mogil, R. J., C. L. Patton, and D. R. Green. 1987. Cellular subsets involved in cell-mediated immunity to murine *Plasmodium yoelii* 17X malaria. *J. Immunol.* 138: 1933–1939.
6. Vinetz, J. M., S. Kumar, M. F. Good, B. J. Fowlkes, J. A. Berzofsky, and L. H. Miller. 1990. Adoptive transfer of CD8$^+$ T cells from immune animals does not transfer immunity to blood stage *Plasmodium yoelii* malaria. *J. Immunol.* 144: 1069–1074.
7. Yanez, D. M., D. D. Manning, A. J. Cooley, W. P. Weidanz, and H. C. van der Heyde. 1996. Participation of lymphocyte subpopulations in the pathogenesis of experimental murine cerebral malaria. *J. Immunol.* 157: 1620–1624.
8. Belnoue, E., M. Kayibanda, A. M. Vigario, J. C. Deschemin, N. van Rooijen, M. Viguier, G. Snounou, and L. Renia. 2002. On the pathogenic role of brain-sequestered $\alpha\beta$ CD8$^+$ T cells in experimental cerebral malaria. *J. Immunol.* 169: 6369–6375.
9. Nitcheu, J., O. Bonduelle, C. Combadiere, M. Tefit, D. Seilhean, D. Mazier, and B. Combadiere. 2003. Perforin-dependent brain-infiltrating cytotoxic CD8$^+$ T lymphocytes mediate experimental cerebral malaria pathogenesis. *J. Immunol.* 170: 2221–2228.
10. Schofield, L., and G. E. Grau. 2005. Immunological processes in malaria pathogenesis. *Nat. Rev. Immunol.* 5: 722–735.
11. Renia, L., S. M. Potter, M. Mauduit, D. S. Rosa, M. Kayibanda, J. C. Deschemin, G. Snounou, and A. C. Gruner. 2006. Pathogenic T cells in cerebral malaria. *Int. J. Parasitol.* 36: 547–554.
12. Heath, W. R., G. T. Belz, G. M. Behrens, C. M. Smith, S. P. Forehan, I. A. Parish, G. M. Davey, N. S. Wilson, F. R. Carbone, and J. A. Villadangos. 2004. Cross-presentation, dendritic cell subsets, and the generation of immunity to cellular antigens. *Immunol. Rev.* 199: 9–26.
13. Rock, K. L., and L. Shen. 2005. Cross-presentation: underlying mechanisms and role in immune surveillance. *Immunol. Rev.* 207: 166–183.
14. Huang, A. Y., A. T. Bruce, D. M. Pardoll, and H. I. Levitsky. 1996. In vivo cross-priming of MHC class I-restricted antigens requires the TAP transporter. *Immunity* 4: 349–355.
15. Gromme, M., F. G. Uytdehaag, H. Janssen, J. Calafat, R. S. van Binnendijk, M. J. Kenter, A. Tulp, D. Verwoerd, and J. Neefjes. 1999. Recycling MHC class I molecules and endosomal peptide loading. *Proc. Natl. Acad. Sci. USA* 96: 10326–10331.
16. Pfeifer, J. D., M. J. Wick, R. L. Roberts, K. Findlay, S. J. Normark, and C. V. Harding. 1993. Phagocytic processing of bacterial antigens for class I MHC presentation to T cells. *Nature* 361: 359–362.
17. Sigal, L. J., S. Crotty, R. Andino, and K. L. Rock. 1999. Cytotoxic T-cell immunity to virus-infected non-haematopoietic cells requires presentation of exogenous antigen. *Nature* 398: 77–80.
18. Mazzaccaro, R. J., M. Gedde, E. R. Jensen, H. M. van Santen, H. L. Ploegh, K. L. Rock, and B. R. Bloom. 1996. Major histocompatibility class I presentation of soluble antigen facilitated by *Mycobacterium tuberculosis* infection. *Proc. Natl. Acad. Sci. USA* 93: 11786–11791.
19. Gubbels, M. J., B. Striepen, N. Shastri, M. Turkoz, and E. A. Robey. 2005. Class I major histocompatibility coplex presentation of antigens that escape from the parasitophorous vacuole of *Toxoplasma gondii*. *Infect. Immun.* 73: 703–711.
20. Bertholet, S., R. Goldszmid, A. Morrot, A. Debrabant, F. Afrin, C. Collazo-Custodio, M. Houde, M. Desjardins, A. Sher, and D. Sacks. 2006. *Leishmania* antigens are presented to CD8$^+$ T cells by a transporter associated with antigen processing-independent pathway in vitro and in vivo. *J. Immunol.* 177: 3525–3533.
21. Ruedl, C., T. Storni, F. Lechner, T. Bachi, and M. F. Bachmann. 2002. Cross-presentation of virus-like particles by skin-derived CD8$^+$ dendritic cells: a dispensable role for TAP. *Eur. J. Immunol.* 32: 818–825.
22. van Dijk, M. R., A. P. Waters, and C. J. Janse. 1995. Stable transfection of malaria parasite blood stages. *Science* 268: 1358–1362.
23. Hogquist, K. A., S. C. Jameson, W. R. Heath, J. L. Howard, M. J. Bevan, and F. R. Carbone. 1994. T cell receptor antagonist peptides induce positive selection. *Cell* 76: 17–27.
24. Van Kaer, L., P. G. Ashton-Rickardt, H. L. Ploegh, and S. Tonegawa. 1992. TAP1 mutant mice are deficient in antigen presentation, surface class I molecules, and CD4$^-$8$^+$ T cells. *Cell* 71: 1205–1214.
25. Shinkai, Y., G. Rathbun, K. P. Lam, E. M. Oltz, V. Stewart, M. Mendelsohn, J. Charron, M. Datta, F. Young, A. M. Stall, et al. 1992. RAG-2-deficient mice lack mature lymphocytes owing to inability to initiate V(D)J rearrangement. *Cell* 68: 855–867.
26. Pircher, H., K. Burki, R. Lang, H. Hengartner, and R. M. Zinkernagel. 1989. Tolerance induction in double specific T-cell receptor transgenic mice varies with antigen. *Nature* 342: 559–561.
27. Miu, J., A. J. Mitchell, M. Muller, S. L. Carter, P. M. Manders, J. A. McQuillan, B. M. Saunders, H. J. Ball, B. Lu, I. L. Campbell, and N. H. Hunt. 2008. Chemokine gene expression during fatal murine cerebral malaria and protection due to CXCR3 deficiency. *J. Immunol.* 180: 1217–1230.
28. Tominaga, N., K. Ohkusu-Tsukada, H. Udono, R. Abe, T. Matsuyama, and K. Yui. 2003. Development of Th1 and not Th2 immune responses in mice lacking IFN-regulatory factor-4. *Int. Immunol.* 15: 1–10.
29. Amante, F. H., A. C. Stanley, L. M. Randall, Y. Zhou, A. Haque, K. McSweeney, A. P. Waters, C. J. Janse, M. F. Good, G. R. Hill, and C. R. Engwerda. 2007. A role for natural regulatory T cells in the pathogenesis of experimental cerebral malaria. *Am. J. Pathol.* 171: 548–559.
30. Wilson, N. S., G. M. Behrens, R. J. Lundie, C. M. Smith, J. Waithman, L. Young, S. P. Forehan, A. Mount, R. J. Steptoe, K. D. Shortman, T. F. de Koning-Ward, et al. 2006. Systemic activation of dendritic cells by Toll-like receptor ligands or malaria infection impairs cross-presentation and antiviral immunity. *Nat. Immunol.* 7: 165–172.
31. Mohan, K., P. Moulin, and M. M. Stevenson. 1997. Natural killer cell cytokine production, not cytotoxicity, contributes to resistance against blood-stage *Plasmodium chabaudi* AS infection. *J. Immunol.* 159: 4990–4998.
32. Doolan, D. L., and S. L. Hoffman. 1999. IL-12 and NK cells are required for antigen-specific adaptive immunity against malaria initiated by CD8$^+$ T cells in the *Plasmodium yoelii* model. *J. Immunol.* 163: 884–892.
33. Hansen, D. S., M. A. Siomos, L. Buckingham, A. A. Scalzo, and L. Schofield. 2003. Regulation of murine cerebral malaria pathogenesis by CD1d-restricted NKT cells and the natural killer complex. *Immunity* 18: 391–402.
34. Slifka, M. K., R. R. Pagarigan, and J. L. Whitton. 2000. NK markers are expressed on a high percentage of virus-specific CD8$^+$ and CD4$^+$ T cells. *J. Immunol.* 164: 2009–2015.
35. Amani, V., M. I. Boubou, S. Pied, M. Marussig, D. Walliker, D. Mazier, and L. Renia. 1998. Cloned lines of *Plasmodium berghei* ANKA differ in their abilities to induce experimental cerebral malaria. *Infect. Immun.* 66: 4093–4099.
36. Urban, B. C., D. J. Ferguson, A. Pain, N. Willcox, M. Plebanski, J. M. Austyn, and D. J. Roberts. 1999. *Plasmodium falciparum*-infected erythrocytes modulate the maturation of dendritic cells. *Nature* 400: 73–77.
37. Ocana-Morgner, C., M. M. Mota, and A. Rodriguez. 2003. Malaria blood stage suppression of liver stage immunity by dendritic cells. *J. Exp. Med.* 197: 143–151.
38. Sponaas, A. M., E. T. Cadman, C. Voisine, V. Harrison, A. Boonstra, A. O'Garra, and J. Langhorne. 2006. Malaria infection changes the ability of splenic dendritic cell populations to stimulate antigen-specific T cells. *J. Exp. Med.* 203: 1427–1433.
39. Caramalho, I., T. Lopes-Carvalho, D. Ostler, S. Zelenay, M. Haury, and J. Demengeot. 2003. Regulatory T cells selectively express Toll-like receptors and are activated by lipopolysaccharide. *J. Exp. Med.* 197: 403–411.
40. Komai-Koma, M., L. Jones, G. S. Ogg, D. Xu, and F. Y. Liew. 2004. TLR2 is expressed on activated T cells as a costimulatory receptor. *Proc. Natl. Acad. Sci. USA* 101: 3029–3034.
41. Imanishi, T., H. Hara, S. Suzuki, N. Suzuki, S. Akira, and T. Saito. 2007. Cutting edge: TLR2 directly triggers Th1 effector functions. *J. Immunol.* 178: 6715–6719.
42. Krishnegowda, G., A. M. Hajjar, J. Zhu, E. J. Douglass, S. Uematsu, S. Akira, A. S. Woods, and D. C. Gowda. 2005. Induction of proinflammatory responses in macrophages by the glycosylphosphatidylinositols of *Plasmodium falciparum*: cell signaling receptors, glycosylphosphatidylinositol (GPI) structural requirement, and regulation of GPI activity. *J. Biol. Chem.* 280: 8606–8616.
43. Omer, F. M., and E. M. Riley. 1998. Transforming growth factor β production is inversely correlated with severity of murine malaria infection. *J. Exp. Med.* 188: 39–48.
44. Ocana-Morgner, C., K. A. Wong, F. Lega, J. Dotor, F. Borras-Cuesta, and A. Rodriguez. 2007. Role of TGF-β and PGE2 in T cell responses during *Plasmodium yoelii* infection. *Eur. J. Immunol.* 37: 1562–1574.
45. Stevenson, M. M., and E. M. Riley. 2004. Innate immunity to malaria. *Nature Rev. Immunol.* 4: 169–180.
46. Nakanishi, K. 2001. Innate and acquired activation pathways in T cells. *Nat. Immunol.* 2: 140–142.

Interferon regulatory factor 4 differentially regulates the production of Th2 cytokines in naïve vs. effector/memory CD4$^+$ T cells

Kiri Honma*, Daisuke Kimura*, Norio Tominaga*, Mana Miyakoda*, Toshifumi Matsuyama†, and Katsuyuki Yui*‡

Divisions of *Immunology and †Cytokine Signaling, Department of Molecular Microbiology and Immunology, Graduate School of Biomedical Sciences, Nagasaki University, Nagasaki 852-8523, Japan

Edited by Tak Wah Mak, University of Toronto, Toronto, ON Canada, and approved August 27, 2008 (received for review April 1, 2008)

Interferon regulatory factor (IRF) 4 is a member of the IRF family of transcription factors and plays critical roles in the development of CD4$^+$ T cells into Th2 and Th17 cells. Using the infection model of *Nippostrongyrus brasiliensis*, we have confirmed the critical roles of IRF-4 in Th2 development *in vivo* by using IRF-4$^{-/-}$ BALB/c mice. However, naïve IRF-4$^{-/-}$CD4$^+$ T cells produced Th2 cytokines, including IL-4, IL-5, and IL-10, but not IL-2 or IFN-γ, at levels higher than wild-type BALB/c CD4$^+$ T cells in response to T cell receptor stimulation. In contrast, effector/memory IRF-4$^{-/-}$CD4$^+$ T cells did not exhibit increased production of Th2 cytokines. Knockdown of IRF-4 expression by using small interfering RNA promoted IL-4 production in naïve CD4$^+$ T cells but inhibited it in effector/memory CD4$^+$ T cells. These results indicate that IRF-4 plays differential roles in the regulation of Th2 cytokine production in naïve CD4$^+$ T cells and effector/memory CD4$^+$ T cells. IRF-4 inhibits Th2 cytokine production in naïve CD4$^+$ T cells, whereas it promotes Th2 cytokine production in effector/memory CD4$^+$ T cells.

siRNA | IL-4 | *Nippostrongyrus brasiliensis*

CD4$^+$ T cells play critical roles in the generation of protective immunity against a variety of pathogens by dictating the type of immune response that is effective against each pathogen encountered. The three types of effector CD4$^+$ T cells, Th1, Th2, and Th17, are characterized by their ability to produce signature cytokines IFN-γ, IL-4, and IL-17, respectively (1, 2). Th2 cells produce IL-4, IL-5, and IL-13 and are responsible for humoral immunity and host immune responses against extracellular parasites. Differentiation of helper T cells is determined after encounter of naïve CD4$^+$ T cells with antigen (3, 4). Initiation of Th2 differentiation is potentiated by IL-4 during encounter of naïve CD4$^+$ T cells with antigen, but the early source of IL-4 that is important for Th2 differentiation under physiological conditions is unclear (5). Although innate immune cells such as basophils and natural killer (NK) T cells can produce IL-4, it has been shown that Th2 cells can develop from naïve CD4$^+$ T cells independently of IL-4 produced by non-T cells (6). Naïve CD4$^+$ T cells themselves can produce small amounts of IL-4 after antigen stimulation, which is sufficient for Th2 differentiation under certain conditions (7). Therefore, IL-4 production by naïve CD4$^+$ T cells must be tightly regulated to coordinate differentiation of effector helper CD4$^+$ T cells. Differentiation of helper CD4$^+$ T cells to Th1 or Th2 is genetically controlled, and the BALB/c strain possesses a genetic predisposition toward the development of Th2 cells (8). These strain differences appear to be controlled at several different levels, and the underlying mechanisms are not clearly understood (9–11).

IFN regulatory factors (IRFs) are a family transcription factors that bind to a specific DNA motif known as the IFN-stimulated response element (ISRE) and play critical roles in a variety of immune processes (12). One of the members, IRF-4, is expressed specifically in lymphocytes and macrophage/dendritic cells (13–17). In contrast to other IRF family members, the expression of IRF-4 in lymphocytes is induced by stimulation of the antigen receptor and plays critical roles for the differentiation of naïve lymphocytes to effectors (13, 18). In T cells, IRF-4 plays a critical role in the differentiation of CD4$^+$ T cells to Th2 and Th17 effectors (19–22). However, IRF-4 is dispensable for Th1 development of CD4$^+$ T cells, and IRF-4$^{-/-}$CD4$^+$ T cells can develop protective immunity during the early phase of *Leishmania major* infection. In these studies, IRF-4$^{-/-}$ mice of C57BL/6 (B6) genetic background, a Th1-biased strain, were used, and it was not clear whether mice with a Th2-biased genetic background also show defects in Th2 development in the absence of the IRF-4 gene.

To examine the role of IRF-4 in effector T cell development under a Th2-biased genetic background, we have backcrossed IRF-4$^{-/-}$ mice to the BALB/c strain. These mice did not develop Th2 immune responses even under strong Th2-biased conditions. Surprisingly, however, naïve IRF-4$^{-/-}$CD4$^+$ T cells produced Th2 cytokines at levels much higher than BALB/c wild-type T cells, suggesting that IRF-4 negatively regulates production of IL-4 in naïve CD4$^+$ T cells. Further study showed that IRF-4 plays differential roles in the regulation of Th2 cytokine production by naïve vs. effector/memory CD4$^+$ T cells. IRF4 inhibits IL-4 production in naïve CD4$^+$ T cell, whereas it promotes IL-4 production in effector/memory CD4$^+$ T cells.

Results

IRF-4$^{-/-}$ Mice Are Sensitive to *Nippostrongyrus brasiliensis* Infection. IRF-4 knockout (KO) mice were backcrossed to BALB/c mice (IRF-4$^{-/-}$ mice) to examine the role of IRF-4 in T cell function under a Th2-biased genetic background. We investigated the response of BALB/c and IRF-4$^{-/-}$ mice to infection with *N. brasiliensis*, which normally induces strong Th2-biased immune responses. In BALB/c mice, expulsion of the adult worms occurred within 2 weeks after infection. In contrast, IRF-4$^{-/-}$ mice maintained similar numbers of intestinal worms for >3 weeks (Fig. 1*A*). In addition, IRF-4$^{-/-}$ mice did not show any signs of eosinophilia, a hallmark of the Th2 response, during the course of *N. brasiliensis* infection, whereas BALB/c mice exhibited eosinophilia with a peak at 2 weeks after infection (Fig. 1*B*). Expulsion of intestinal adult worms is critically dependent on IL-4 and IL-13 produced by T cells (23, 24). CD4$^+$ T cells were prepared from the draining lymph nodes of the infected mice,

Author contributions: K.H. and K.Y. designed research; K.H., D.K., and N.T. performed research; T.M. contributed new reagents/analytic tools; K.H., D.K., N.T., M.M., and K.Y. analyzed data; and K.H. and K.Y. wrote the paper.

The authors declare no conflict of interest.

This article is a PNAS Direct Submission.

‡To whom correspondence should be addressed at: Division of Immunology, Department of Molecular Microbiology and Immunology, Graduate School of Biomedical Sciences, Nagasaki University, 1-12-4 Sakamoto, Nagasaki 852-8523, Japan. E-mail: katsu@nagasaki-u.ac.jp.

This article contains supporting information online at www.pnas.org/cgi/content/full/0803171105/DCSupplemental.

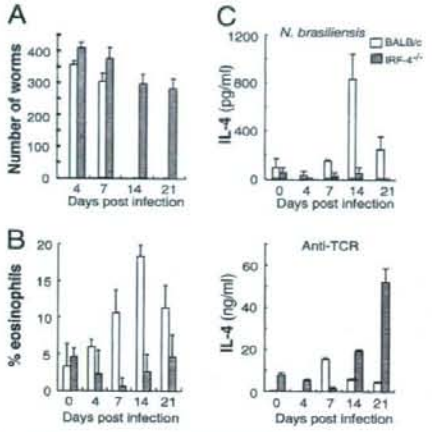

Fig. 1. IRF-4$^{-/-}$ mice are susceptible to *N. brasiliensis* infection. (*A*) BALB/c (open bars) and IRF-4$^{-/-}$ mice (filled bars) were infected with *N. brasiliensis* (500 organisms) s.c. at the base of the tail. Worm burden was analyzed after longitudinal dissection of the small intestine. The data represent the mean ± SD with three mice per group. (*B*) Eosinophils in the peripheral blood were counted under a microscope. (*C*) Mesenteric lymph node cells (1×10^5) were collected on the indicated days after infection and were cultured in the presence of *N. brasiliensis* antigen (*Upper*) or on plates coated with anti-TCR mAb (*Lower*) for 48 h. The IL-4 levels in the supernatant were determined by ELISA. Representative results of three independent experiments are shown.

and their ability to produce IL-4 was determined by ELISA. CD4$^+$ T cells of BALB/c mice produced IL-4 in response to *N. brasiliensis* antigen, whereas those from IRF-4$^{-/-}$ mice did not (Fig. 1*C*). The lack of IL-4 production was not caused by a defect in antigen presentation by IRF-4$^{-/-}$ antigen-presenting cells (APCs) during the culture because IRF-4$^{-/-}$CD4$^+$ T cells did not produce IL-4 when cultured with wild-type BALB/c APCs pulsed with *N. brasiliensis* antigen (data not shown). In addition, IRF-4$^{-/-}$ mice showed Th1-based protective immune responses against infection with *L. major* [supporting information (SI) Fig. S1]. Collectively, these studies established that the Th2 response *in vivo* is critically dependent on IRF-4, even in mice genetically biased to Th2.

IRF-4$^{-/-}$CD4$^+$ T Cells Produce High Levels of Th2 Cytokines. During the course of the study, we evaluated the ability of CD4$^+$ T cells to produce IL-4 in response to anti-T cell receptor (TCR) signals. Unexpectedly, CD4$^+$ T cells from IRF-4$^{-/-}$ mice produced IL-4 at levels higher than that produced by CD4$^+$ T cells from BALB/c mice when stimulated with anti-TCR mAb despite the lack of their antigen-specific IL-4 production (Fig. 1*C*). Therefore, we examined whether conventional CD4$^+$ T cells expressing α/β TCR that recognize MHC/peptide antigens mediate the high IL-4 responses. CD4$^+$ T cells from BALB/c and IRF-4$^{-/-}$ mice were stimulated with APC pulsed with staphylococcal enterotoxin B (SEB) or with plate-coated anti-TCR mAb, and their ability to produce cytokines was determined (Fig. 2*A*). IRF-4$^{-/-}$CD4$^+$ T cells produced IL-2 and IFN-γ at levels lower than BALB/c CD4$^+$ T cells, consistent with previous studies (18, 20, 21). These T cells, however, produced IL-4 and IL-5 at levels much higher than BALB/c CD4$^+$ T cells when stimulated with SEB-pulsed APC or anti-TCR mAb (Fig. 2*A*). To determine whether conventional CD4$^+$ T cells or NK T cells produce high levels of IL-4 and IL-5, we stimulated these cells with staphylococcal enterotoxin A (SEA), which stimulates T cells expressing Vβ1, 3 10, 11, 12, and 17; or with α-galactocylceramide (α-GalCer), which stimulates Vα14$^+$ NK T cells to determine whether conventional CD4$^+$ T cells or NK T cells produce high levels of IL-4 and IL-5 (Fig. 2*B*) (25). IRF-4$^{-/-}$CD4$^+$ T cells produced higher levels of IL-4 and lower levels IL-2 and IFN-γ in response to SEA compared with BALB/c CD4$^+$ T cells. To confirm that IRF-4$^{-/-}$ naïve conventional CD4$^+$ T cells produce

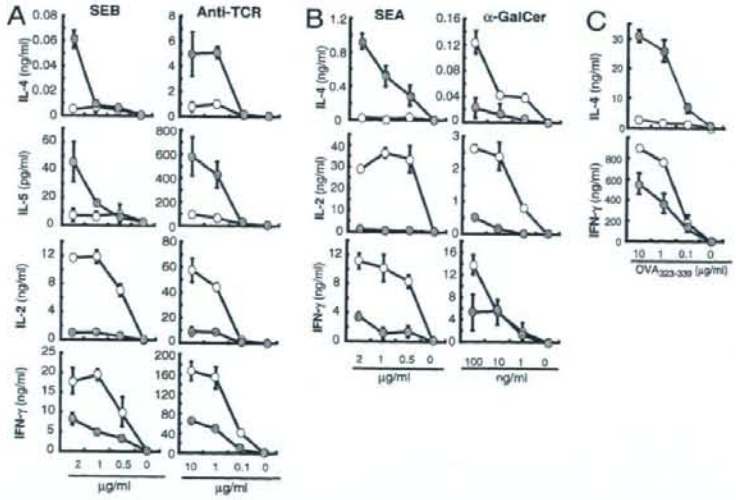

Fig. 2. Conventional CD4$^+$ T cells from IRF-4$^{-/-}$ mice produce IL-4 at levels higher than wild-type CD4$^+$ T cells. (*A*) Splenic CD4$^+$ T cells (1×10^5) from BALB/c (open circles) or IRF-4$^{-/-}$ (closed circles) mice were cultured with mitomycin C-treated T-depleted spleen cells (5×10^5) pulsed with SEB or on plates coated with anti-TCR Ab for 48 h at the indicated concentrations. The cytokine levels in the supernatant were determined by ELISA. (*B*) Splenic CD4$^+$ T cells (2×10^5) from BALB/c (open circles) or IRF-4$^{-/-}$ (filled circles) mice were cultured in the presence of mitomycin C-treated T-depleted spleen cells (5×10^5) and SEA or α-GalCer at the indicated concentrations for 48 h. (*C*) Naïve CD4$^+$ T cells (1×10^5 CD62L$^+$CD4$^+$ T cells) from DO11.10 (open circles) or IRF-4$^{-/-}$ DO11.10 (closed circles) mice were stimulated with mitomycin C-treated T-depleted spleen cells (4×10^5) in the presence of $OVA_{323-339}$ peptide (0–10 μg/ml) for 48 h. Representative results of three independent experiments are shown.

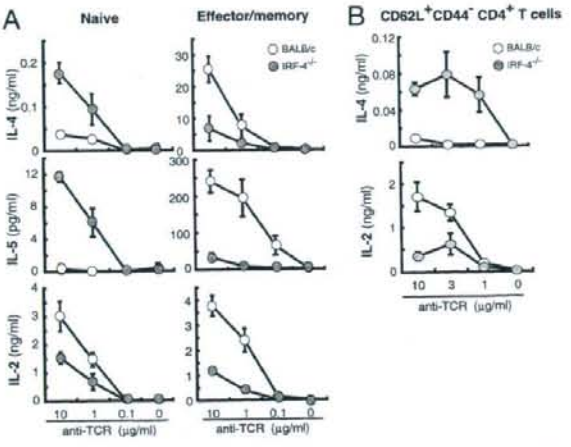

Fig. 3. Th2 cytokine production by naïve vs. effector/memory CD4$^+$ T cells is differentially regulated in IRF-4$^{-/-}$ mice. (*A*) Naïve (CD62L$^+$) or effector/memory (CD62L$^-$) CD4$^+$ T cells (1×10^5 per well) from BALB/c (open circles) or IRF-4$^{-/-}$ (filled circles) mice were purified by sorting and were cultured with plates coated with anti-TCR mAb for 48 h. The percentage of CD62L$^+$ cells and CD62L$^-$ cells within BALB/c and IRF-4$^{-/-}$CD4$^+$ T cells was 97–99% and >99%, respectively. Cytokine levels in the supernatant were determined by ELISA. Representative results of three independent experiments are shown. (*B*) CD62L$^+$CD44$^-$CD4$^+$ T cells (2×10^5) from BALB/c (open circles) or IRF-4$^{-/-}$ (filled circles) mice were purified by sorting and were cultured on plates coated with anti-TCR mAb for 48 h. The purity of CD62L$^+$CD44$^-$CD4$^+$ T cells was >92%.

higher levels of IL-4, we have backcrossed DO11.10 TCR transgenic mice with IRF-4$^{-/-}$BALB/c mice and examined the cytokine production of naïve DO11.10 IRF-4$^{-/-}$CD4$^+$ T cells in response to APC pulsed with $OVA_{323-339}$ peptide. These T cells produced higher levels of IL-4 and reduced levels of IFN-γ in response to $OVA_{323-339}$ peptide (Fig. 2*C*), indicating that conventional IRF-4$^{-/-}$CD4$^+$ T cells produced IL-4 at high levels in response to TCR stimulation. In contrast, total CD4$^+$ cells from IRF-4$^{-/-}$ mice produced IL-4, IL-2, and IFN-γ at reduced levels in response to α-GalCer (Fig. 2*B*). The proportion of CD4$^+$ NK T cells (DX5$^+$ cells) in IRF-4$^{-/-}$ mice was lower than BALB/c mice (Fig. S2), partly explaining the reduced IL-4 production of CD4$^+$ cells from IRF-4$^{-/-}$ mice in response to α-GalCer (Fig. 2*B*). Purified CD4$^+$DX5$^+$ cells from IRF-4$^{-/-}$ mice, however, produced equivalent or higher levels of IL-4 in response to α-GalCer than those from BALB/c mice (Fig. S2), suggesting that IRF-4$^{-/-}$CD4$^+$DX5$^+$ NK T cells are able to produce sufficient levels of IL-4 in response to α-GalCer.

IL-4 Production by Naïve vs. Effector/Memory IRF-4$^{-/-}$CD4$^+$ T Cells. Peripheral CD4$^+$ T cells contain both naïve and effector/memory-type T cells that can be distinguished by their cell surface phenotype such as CD62L. Naïve lymphocytes have higher levels of CD62L expression than effector and effector memory T cells (26). The proportion of CD62L$^+$ cells in CD4$^+$ T cells was not significantly different between BALB/c and IRF-4$^{-/-}$ mice (data not shown). To determine which cell type produces higher levels of Th2 cytokines in IRF-4$^{-/-}$ mice, we prepared naïve (CD62L$^+$) and effector/memory (CD62L$^-$) CD4$^+$ T cells and examined their cytokine production in response to anti-TCR mAb (Fig. 3*A*). Naïve IRF-4$^{-/-}$CD4$^+$ T cells produced IL-4 and IL-5 at levels higher than BALB/c naïve CD4$^+$ T cells and IL-2 at reduced levels. Effector/memory CD4$^+$ T cells from IRF-4$^{-/-}$ BALB/c mice, however, produced IL-4, IL-5, and IL-2 at levels lower than BALB/c CD4$^+$ T cells. CD62L$^+$CD4$^+$ T cell population may contain central memory CD4$^+$ T cells (CD62L$^+$CD44$^+$) in addition to naïve CD4$^+$ T cells (CD62L$^+$CD44$^-$). To confirm that naïve CD4$^+$ T cells produce higher levels of IL-4, we purified CD62L$^+$CD44$^-$CD4$^+$ T cells by sorting and cultured in the presence of anti-TCR mAb (Fig. 3*B*). CD62L$^+$CD44$^-$CD4$^+$ T cells from IRF-4$^{-/-}$ mice produced IL-4 at levels higher than those BALB/c mice and IL-2 at reduced levels. Thus, we concluded that naïve IRF-4$^{-/-}$CD4$^+$ T cells rather than effector/memory IRF-4$^{-/-}$CD4$^+$ T cells were responsible for the high levels of Th2 cytokines produced. We also determined the expression of Th2 cytokine mRNAs by naïve CD4$^+$ T cells (Fig. S3). The expression levels of cytokine mRNA were detected basically in parallel to their protein production. Also, up-regulation of GATA3 mRNA expression was observed in naïve IRF-4$^{-/-}$CD4$^+$ T cells and not in BALB/c CD4$^+$ T cells. Taken together, these results suggest that IRF-4 plays an inhibitory role in the expression of Th2 cytokines in naïve T cells. This inhibitory effect, however, was not seen in effector/memory-type CD4$^+$ T cells.

To examine the mechanisms underlying the differential effect of IRF-4 in naïve and effector/memory T cells, we compared the expression levels of IRF-4 in BALB/c CD4$^+$ T cells after stimulation with anti-TCR mAb. Naïve (CD62L$^+$) CD4$^+$ T cells expressed IRF-4 protein at a level significantly higher than effector/memory (CD62L$^-$) CD4$^+$ T cells (Fig. 4*A*). We examined the kinetics of IRF-4 expression after T cell activation both at the RNA and protein levels (Fig. 4 *B* and *C*). The expression of IRF-4 was induced after activation with TCR stimulation in both naïve and effector/memory CD4$^+$ T cells. Compared with effector/memory CD4$^+$ T cells, however, naïve CD4$^+$ T cells showed higher levels of IRF-4 mRNA expression at early hours after TCR stimulation. Similarly, intracellular staining of IRF-4 protein indicated that the expression of IRF-4 was induced at higher levels in naïve CD4$^+$ cells than effector/memory CD4$^+$ cells during the early time point after activation (Fig. 4*C*). In contrast, the expression of IRF-1 was not induced in naïve CD4$^+$ T cells and was only transiently increased in effector/memory CD4$^+$ T cells (Fig. 4*B*). These results indicate that the expression pattern of IRF-4 after T cell activation is distinct in naïve and effector/memory CD4$^+$ cells.

Regulation of Th2 Cytokine Production by IRF-4. To determine whether the ability of CD4$^+$ T cells to express Th2 cytokines is directly regulated by IRF-4, we reconstituted the IRF-4 gene in IRF-4$^{-/-}$CD4$^+$ T cells by transfection. CD4$^+$ T cells reconstituted with IRF-4 produced reduced levels of IL-4 and IL-5 in response to anti-TCR mAb (Fig. S4). We next used the siRNA technique to inhibit expression of IRF-4 in CD4$^+$ T cells. Naïve CD4$^+$ T cells were prepared by depletion of CD44^{high} cells from total CD4$^+$ T cells. After transfer of IRF-4 siRNA by electroporation, cells were stimulated with anti-TCR mAb. Naïve CD4$^+$ T cells expressing greatly decreased levels of IRF-4 produced IL-4 at levels much higher than control CD4$^+$ T cells in response to TCR stimulation at both the RNA and protein levels (Fig. 5 *A* and *B*). We also evaluated the effect of inhibiting IRF-4 expression in effector/memory CD4$^+$ T cells because these cells normally produce IL-4 at levels higher than IRF-4$^{-/-}$ effector/memory CD4$^+$ T cells. Effector/memory CD4$^+$ T cells were prepared by depletion of CD62L$^+$ cells from total CD4$^+$ T cells, transfected with IRF-4 siRNA, and stimulated with anti-TCR mAb. The production of IL-4 by effector/memory CD4$^+$ T cells was significantly inhibited by IRF-4-specific siRNA at both protein and RNA levels (Fig. 5 *C* and *D*). These results suggest that IRF-4 expressed in CD4$^+$ T cells differentially regulates Th2 cytokine production in naïve and effector/memory CD4$^+$ T cells. IRF-4 is inhibitory to IL-4 production in naïve CD4$^+$ T cells and is stimulatory in effector/memory CD4$^+$ T cells.

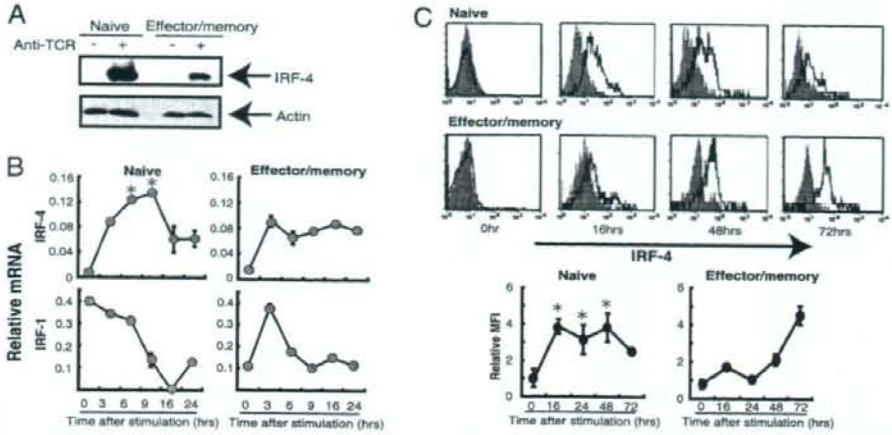

Fig. 4. Induction of IRF-4 expression in naïve and effector/memory CD4$^+$ T cells after TCR stimulation. (*A*) CD62L$^+$ and CD62L$^-$CD4$^+$ T cells were prepared from BALB/c mice and were cultured on plates coated with or without anti-TCR mAb (1 μg/ml for *A* and *B*, 10 μg/ml for *C*). After culture for 16 h, cells were lysed, separated on 12.5% SDS/PAGE, blotted, and probed with anti-IRF-4 Ab. The membrane was stripped and reprobed with anti-actin Ab. (*B*) After culture for 0–24 h, total RNA was prepared, and the levels of IRF mRNA were determined by real-time PCR. The mRNA expression was expressed as the ratio of DNA to G3PDH. *, $P < 0.05$, Mann–Whitney *U* test between naïve and effector/memory. (*C*) After culture for 0–72 h, cells were fixed, permeabilized, and stained with anti-IRF-4 Ab, biotin-anti-goat IgG, and streptavidin–phycoerythrin. Gray shadow represents staining of the cells at each time point with biotinylated anti-goat IgG and streptavidin–phycoerythrin only without anti-IRF-4 Ab. Relative mean fluorescent intensity (MFI) of IRF-4 staining was expressed as the ratio of MFI between the staining with and without anti-IRF-4 Ab. Representative results of three independent experiments are shown. *, $P < 0.05$ between naïve and effector/memory.

Discussion

We have shown a complete lack of Th2-type immune responses *in vivo* in IRF-4$^{-/-}$ mice of BALB/c genetic background. IRF-4$^{-/-}$ mice were unable to expel *N. brasiliensis in vivo* because of the lack of Th2-type effector cells. These results are consist with our previous reports using IRF-4 KO mice on a B6 background, in which we and others showed *in vitro* that Th2 responses of IRF4$^{-/-}$CD4$^+$ B6 T cells were impaired (19–21). Rengarajan *et al.* (19) described that IRF-4 physically interacts with NFATc2 and enhances transcriptional activation of the IL-4 promoter. In human studies, Hu *et al.* (27) reported that stable expression of IRF-4 in the Jurkat human T cell line led to production of Th2 cytokines and that IRF-4 binds the IL-4 promoter element triggering the transcription of IL-4. These studies used immortalized cells, which may represent effector/memory cell types, to evaluate the effect of IRF-4 on IL-4 production, and they are consistent with our observation that IRF-4$^{-/-}$CD4$^+$ T cells are defective in Th2 development and that IL-4 production by effector/memory IRF-4$^{-/-}$CD4$^+$ T cells is much lower than BALB/c CD4$^+$ T cells. This work, however, has added a finding that IRF-4 has an inhibitory effect on the production of Th2 cytokines by naïve CD4$^+$ T cells in response to TCR stimulation. These results are seemingly paradoxical but are consistent with the results of IRF-4 knockdown experiments using siRNA in naïve vs. effector/memory type CD4$^+$ T cells; the inhibition of IRF-4 expression in naïve CD4$^+$ T cells conferred the ability to produce IL-4 on naïve CD4$^+$ T cells, whereas inhibition of IRF-4 expression in effector/memory CD4$^+$ T cells down-regulated IL-4 expression.

Studies on the function of IRF-4 indicated that it could function as either a transcriptional activator or repressor depending on the context of the DNA-binding sequences and/or protein-interacting partners (14, 19, 28–31). IRF-4 contains an amino-terminal DNA-binding domain and a carboxyl-terminal IRF association domain that can interact with a variety of proteins, including IRFs. IRF-4 interacts with Ets family member PU.1, transcription factor E47, Stat6, Bcl-6 or NFATc2 to synergistically enhance transcriptional activity of a variety of genes including the Ig light chain gene in B cells and IL-4 in T cells (14, 19, 28, 29). However, IRF-4 has been shown to repress gene activation induced by other IRFs and does not appear to require association with other proteins (30, 31). We have shown that IRF-4 inhibits IRF-1-dependent transcription of genes, including *TRAIL*, and that the IRF association domain of IRF-4 was dispensable for this inhibition, suggesting that IRF-4 acts as a natural antagonist of IRF-1 and inhibits its transactivation (31). There are at least three IRF-binding sites located in the IL-4 promoter region, some of which correspond with sequences that negatively regulate IL-4 promoter activity (32, 33). Elser *et al.* (33) showed that IRF-1 and IRF-2 bind to these sites and inhibit IL-4 promoter activity and that naïve IRF-1$^{-/-}$CD4$^+$ T cells produce IL-4 at levels higher than wild type. Because IRF-1 and IRF-2 are induced by IFN-γ, these IRFs were believed to mediate the inhibitory role of IFN-γ on expression of the IL-4 gene. Our study shows that naïve IRF-4$^{-/-}$CD4$^+$ T cells produce higher levels of IL-4 upon TCR stimulation. Therefore, both IRF-4 and IRF-1 appear to be required for optimum inhibition of IL-4 production in naïve CD4$^+$ T cells. Unlike IRF-1 and IRF-2, which are constitutively expressed in T cells, IRF-4 expression is induced by antigen receptor-mediated stimuli (Fig. 4*B*) (13). Thus, IRF-1 and IRF-4 may cooperate temporally to regulate the induction of IL-4 in naïve CD4$^+$ T cells tightly. Taken together, these studies suggest that IRF-4 plays a dual function in the production of IL-4 in CD4$^+$ T cells; IRF-4 promotes IL-4 production in effector/memory CD4$^+$ T cells in association with NFATc2 and inhibits IL-4 transcription in naïve CD4$^+$ T cells. The precise mechanisms underlying the inhibition of IL-4 transcription by IRF-4 remain to be determined.

The question, then, is how the same transcription factor can have two opposing functions in naïve vs. effector/memory CD4$^+$ T cells. One possibility lies in the differential expression levels of IRF-4 in naïve and effector/memory-type CD4$^+$ T cells. IRF-4 expression is induced after activation of T cells through TCR signaling and reaches higher levels in naïve CD4$^+$ T cells than in effector/memory CD4$^+$ T cells. The early and strong induction of IRF-4 may be required for silencing of IL-4 expression.

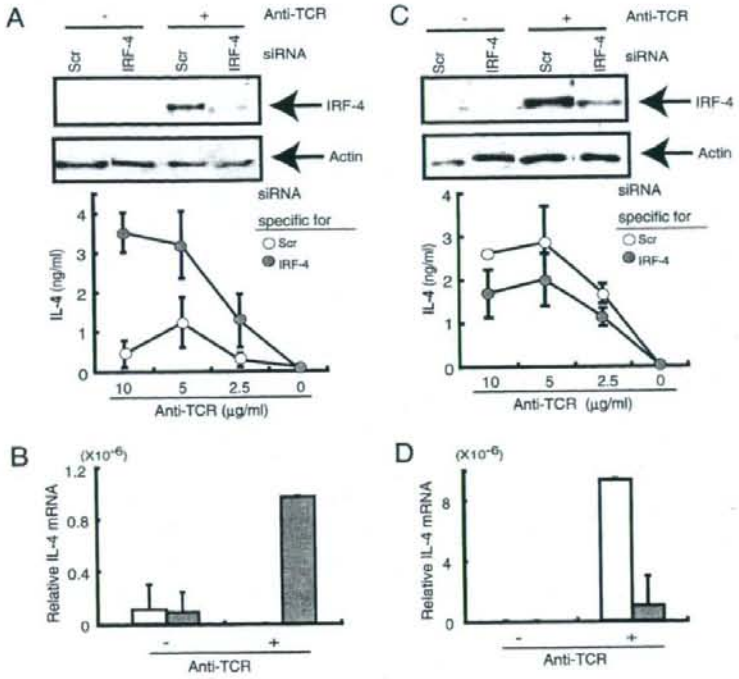

Fig. 5. The levels of IRF-4 expression in CD4$^+$ T cells affect the levels of Th2 cytokine production. Naïve CD4$^+$ T cells (CD44^{low}) (*A* and *B*) and effector/memory CD4$^+$ T cells (CD62L$^-$) (*C* and *D*) from BALB/c mice were transfected with IRF-4-specific (IRF-4) or control (Scr) siRNA (100 pmol). Cells were stimulated with plate-bound anti-TCR mAb for 48 h (*A*), 60 h (*C*), or 4 h (*B* and *D*). The expression of IRF-4 protein was determined by Western blot analysis by using cells stimulated with anti-TCR mAb at the concentrations of 0 (−) and 2.5 (+) μg/ml (*A* and *C*). The blot was stripped and reprobed with anti-actin Ab. The IL-4 levels in the supernatant were determined by ELISA (*A* and *C*). After culture for 4 h on plates coated with anti-TCR mAb (3 μg/ml), RNA was prepared, and the levels of IL-4 were determined by real-time PCR (*B* and *D*).

Second, IRF-4 might affect the signaling of TCR or threshold of T cell activation, which ultimately dictate the differential production of cytokines. This possibility may also explain the lack of Th2 differentiation in IRF-4 KO mice because the strength of TCR signaling appear to affect the generation of Th1/Th2 cells (34). We have reported that IRF-4 regulates the TLR signaling pathway, including the activation of MAP kinases and NF-κB in macrophages (17), and it is possible that IRF-4 affects TCR signaling in T cells. Third, IRF-4 might interact with partners distinct from NFAT, which dictates the repressive function of IRF-4 on the IL-4 promoter in naïve CD4$^+$ T cells. However, IL-4 expression is controlled not only by the IL-4 promoter, but by several other regulatory elements, including enhancers, silencers, and locus control regions, which become targets of transcription factors and chromatin-remodeling factors (3, 4). There are IRF-binding sites within the silencer region (35). Therefore, IRF-4 may affect not only promoter activity of the target genes, but also the chromatin environment of the target genes in regulating gene expression (36). Our study indicates that IRF-4 is involved in regulating the expression of the majority of Th2 cytokines, including IL-4 and IL-5, supporting the view that IRF-4 is involved in the coordinated expression of Th2 cytokines through influences on chromatin structure. Control of Th2 cytokine expression is brought about by the coordinated actions of IRF-4 and a variety of transcriptional elements and chromatin structure influences.

Taken together, our findings suggested that IRF-4 plays dual roles in Th2 cytokine production in CD4$^+$ T cells. IRF-4 is a negative regulator of Th2 cytokines during the early activation phase of naïve CD4$^+$ T cells, whereas it promotes Th2 development and Th2 cytokine production in effector/memory CD4$^+$ T cells. Th2 T cells are critical for protection against extracellular parasites and for the pathogenesis of allergic immune responses. Our work reveals critical dual roles of IRF-4 in the regulation of Th2 function.

Materials and Methods

Mice and *N. brasiliensis*. IRF-4 KO mice were initially mated to C57BL/6 mice as described (17, 21). IRF-4 KO mice of BALB/c background (IRF-4$^{-/-}$ mice) were generated by backcrossing IRF-4 KO mice onto BALB/c for 10 generations and were maintained by intercrossing. The genotype was determined by PCR as described in ref. 21. DO11.10 mice, provided by M. Kubo (Riken, Yokohama, Japan), were crossed with IRF-4$^{-/-}$ mice to generate IRF-4$^{-/-}$ DO11.10 mice. These mice were maintained by intercrossing in the Laboratory Animal Center for Animal Research at Nagasaki University. C57BL/6 (B6) and BALB/c mice were purchased from Japan SLC Inc. Mice were used at 6–8 weeks old. All animal experiments were conducted with approval from the Nagasaki University Institutional Animal Care Committee. *N. brasiliensis* was provided by K. Ishiwata (Jikei University School of Medicine, Tokyo, Japan). Third-stage larvae (L3) of *N. brasiliensis* were injected into mice s.c. (500 per mouse) at the base of tail as described in ref. 37. Worm burden was analyzed after longitudinal dissection of the small intestine. Blood smear was stained by using Diff-Quik (Sysmex), and eosinophils were counted under a microscope. *N. brasiliensis* antigens were prepared by freezing and thawing.

Infection with *L. major* is discussed in *SI Methods*.

Cell Culture, ELISA, and Flow Cytometry. Mesenteric lymph node cells (1×10^5) were cultured in the presence of *N. brasiliensis* antigen. In other T cell responses, lymphocytes were collected from a mixture of lymph nodes (mesenteric and inguinal) and spleen. CD4$^+$ T cells (>98%) were prepared by using anti-CD4 IMag (BD Biosciences). CD62L$^+$CD4$^+$ T cells were purified by sorting

(purity, 97~99%) by using FACSAria (BD Biosciences) (Fig. 3A) or separated by using the $CD4^+CD62L^+$ isolation kit (purity, 70–80%) (Miltenyi Biotec) (Fig. 4, 5). $CD62L^-CD4^+$ T cells were purified by sorting (purity, >99%, Fig. 3A) or were prepared by treating the negative fraction of $CD4^+CD62L^+$ isolation kit with complement at 37°C for 30 min to deplete the remaining $CD62L^+$ cells (purity, 93–97%, Figs. 4 and 5). T cells were stimulated with plate-bound anti-TCRβ mAb (H57) or mitomycin C-treated T-depleted spleen cells pulsed with α-GalCer (KRN7000, Kirin Brewery), SEA (Toxin Technology), or SEB. Supernatant was collected 48 h after stimulation, and the levels of cytokines in the supernatants were determined by sandwich ELISA. IL-2, IL-4, and IFN-γ levels were determined as described (17, 21). IL-5 levels were determined by an ELISA kit (R&D Systems). We did not find any significant differences in the cytokine profiles between $CD62L^+CD4^+$ or $CD62L^-CD4^+$ T cells that were purified by sorting and those purified by $CD4^+CD62L^+$ isolation kit (data not shown).

For intracellular staining of IRF-4, $CD62L^+CD4^+$ T cells and $CD62L^-CD4^+$ T cells were purified by using a $CD4^+CD62L^+$ isolation kit, stimulated with plate-coated anti-TCR mAb, fixed, and permeabilized by using Cytofix/Cytoperm kits (BD PharMingen), and were stained with anti-IRF-4 Ab (Santa-Cruz Biotechnology), biotin–anti-goat IgG Ab, and phycoerythrin–streptavidin. Cells were analyzed by using FACScan (BD Biosciences) (Fig. 4C).

Real-Time PCR. RNA was prepared from cells by using Isogen (Nippon Gene). Total RNA (500 ng) was reverse-transcribed to cDNA by using random hexamers, and real-time PCR was performed as described in ref. 17. The mRNA expression was determined as the ratio of each DNA to glucose-3-phosphate dehydrogenase. The sequence of primers for GATA3 and Tbet was described in ref. 21. The sequences of other primer pairs are shown in Table S1.

Western Blotting. Cells were washed and resuspended in sample buffer. The lysate was size-fractionated on 12.5% SDS/PAGE and transferred to a PVDF membrane. The blot was blocked with 5% milk TBS–Tween, washed twice with PBS–Tween, and incubated with anti-IRF-4 Ab (Santa Cruz Biotechnology). The membrane was incubated with horseradish peroxidase–anti-goat Ig Ab (MBL), washed, and visualized by using ECL reagent (Amersham Pharmacia). The same blot was stripped and reprobed with anti-actin Ab (Sigma).

Transfection and RNA Interference Assay. Full-length mouse IRF-4 cDNA was cloned into pcDNA3 (Invitrogen). $CD4^+$ T cells were prepared by using $CD4^+$ T cell isolation kit (Miltenyi Biotech) and AutoMACS, and were transfected with the plasmid DNA (30 μg) by using a Nucleofector apparatus (Amaxa) in a 2.0-mm electroporation cuvette according to the protocol X-01. Three hours later, cells (5×10^5) were washed and seeded in 96-well flat-bottom plates coated with anti-TCR Ab and cultured for 48 h.

Double-stranded RNA for IRF-4 and control (22) were purchased from Takara Bio. $CD4^+$ T cells were prepared by using the $CD4^+$ T cells isolation kit (Miltenyi Biotec). Naïve and effector/memory $CD4^+$ T cells were prepared from these cells by negative selection by using biotin–anti-CD44 mAb plus streptavidin–microbeads and FITC–anti-CD62L plus anti-FITC microbeads, respectively, followed by AutoMACS. Cells were transfected with FITC-labeled dsRNA (100 pmol) in a 2.0-mm electroporation cuvette according to the protocol X-01 by using a Nucleofector apparatus, and were cultured on plates coated with anti-TCR mAb for 4–48 h. The proportion of cells that incorporated the dsRNA was ~97% as assessed by flow cytometry.

Statistics. Significance levels were determined by the Mann–Whitney *U* test for unpaired observations. Results were considered significant when $P < 0.05$.

ACKNOWLEDGMENTS. We thank M. Ueda, K. Kimura, T. Ikeda, and M. Yoshida for excellent technical assistance. We also thank Dr. K. Nagai for discussion and help, Dr. K. Ishiwata for *N. brasiliensis*, and Kirin Brewery for α-GalCer. This work was supported by grants-in-aid from the Ministry of Education, Science, Sports, and Culture, Japan, by the 21st Century Center of Excellence program, and by the president's discretionary fund of Nagasaki University, Japan.

1. Mosmann T-R, Coffman R-L (1989) Th1 and Th2 cells: Different patterns of lymphokine secretion lead to different functional properties. *Annu Rev Immunol* 7:145–173.
2. Weaver C-T, Hatton R-D, Mangan P-R, Harrington L-E (2007) IL-17 family cytokines and the expanding diversity of effector T cell lineages. *Annu Rev Immunol* 25:821–852.
3. Ansel K-M, Djuretic I, Tanasa B, Rao A (2006) Regulation of Th2 differentiation and IL4 locus accessibility. *Annu Rev Immunol* 24:607–656.
4. Lee G-R, Kim S-T, Spilianakis C-G, Fields P-E, Flavell RA (2006) T helper cell differentiation: Regulation by cis elements and epigenetics. *Immunity* 24:369–379.
5. O'Garra A (1998) Cytokines induce the development of functionally heterogeneous T helper cell subsets. *Immunity* 8:275–283.
6. Schmitz J, *et al.* (1994) Induction of interleukin 4 (IL-4) expression in T helper (Th) cells is not dependent on IL-4 from non-Th cells. *J Exp Med* 179:1349–1353.
7. Noben-Trauth N, Hu-Li J, Paul WE (2000) Conventional, naïve $CD4^+$ T cells provide an initial source of IL-4 during Th2 differentiation. *J Immunol* 165:3620–3625.
8. Hsieh C-S, Macatonia S-E, O'Garra A, Murphy K-M (1995) T cell genetic background determines default T helper phenotype development *in vitro*. *J Exp Med* 181:713–721.
9. Guler M-L, Jacobson N-G, Gubler U, Murphy K-M (1997) T cell genetic background determines maintenance of IL-12 signaling: Effects on BALB/c and B10.D2 T helper cell type 1 phenotype development. *J Immunol* 159:1767–1774.
10. Bix M, Wang Z-E, Thiel B, Schork N-J, Locksley R-M (1998) Genetic regulation of commitment to interleukin 4 production by a $CD4^+$ T cell-intrinsic mechanism. *J Exp Med* 188:2289–2299.
11. Launois P, *et al.* (1997) IL-4 rapidly produced by $V\beta4V\alpha8$ $CD4^+$ T cells instructs Th2 development and susceptibility to. *Leishmania major* in BALB/c mice. *Immunity* 6:541–549.
12. Taniguchi T, Ogasawara K, Takaoka A, Tanaka N (2001) IRF family of transcription factors as regulators of host defense. *Annu Rev Immunol* 19:623–655.
13. Matsuyama T, *et al.* (1995) Molecular cloning of LSIRF, a lymphoid-specific member of the interferon regulatory factor family that binds the interferon-stimulated response element (ISRE). *Nucleic Acids Res* 23:2127–2136.
14. Eisenbeis C-F, Singh H, Storb U (1995) Pip, a novel IRF family member, is a lymphoid-specific, PU.1-dependent transcriptional activator. *Genes Dev* 9:1377–1387.
15. Marecki S, Atchison M-L, Fenton M-J (1999) Differential expression and distinct functions of IFN regulatory factor 4 and IFN consensus sequence-binding protein in macrophages. *J Immunol* 163:2713–2722.
16. Suzuki S, *et al.* (2004) Critical roles of interferon regulatory factor 4 in $CD11b^{high}CD8\alpha^-$ dendritic cell development. *Proc Natl Acad Sci USA* 101:8981–8986.
17. Honma K, *et al.* (2005) Interferon regulatory factor 4 negatively regulates the production of proinflammatory cytokines by macrophages in response to LPS. *Proc Natl Acad Sci USA* 102:16001–16006.
18. Mittrucker H-W, *et al.* (1997) Requirement for the transcription factor LSIRF/IRF4 for mature B and T lymphocyte function. *Science* 275:540–543.
19. Rengarajan J, *et al.* (2002) Interferon regulatory factor 4 (IRF4) interacts with NFATc2 to modulate interleukin 4 gene expression. *J Exp Med* 195:1003–1012.
20. Lohoff M, *et al.* (2002) Dysregulated T helper cell differentiation in the absence of interferon regulatory factor 4. *Proc Natl Acad Sci USA* 99:11808–11812.
21. Tominaga N, *et al.* (2003) Development of Th1 and not Th2 immune responses in mice lacking IFN-regulatory factor-4. *Int Immunol* 15:1–10.
22. Brustle A, *et al.* (2007) The development of inflammatory T(H)-17 cells requires interferon-regulatory factor 4. *Nat Immunol* 8:958–966.
23. Finkelman F-D, *et al.* (2004) Interleukin-4- and interleukin-13-mediated host protection against intestinal nematode parasites. *Immunol Rev* 201:139–155.
24. Zhao A, *et al.* (2003) Dependence of IL-4, IL-13, and nematode-induced alterations in murine small intestinal smooth muscle contractility on Stat6 and enteric nerves. *J Immunol* 171:948–954.
25. Kawano T, *et al.* (1997) CD1d-restricted and TCR-mediated activation of $V\alpha14$ NKT cells by glycosylceramides. *Science* 278:1626–1629.
26. Seder R-A, Ahmed R (2003) Similarities and differences in $CD4^+$ and $CD8^+$ effector and memory T cell generation. *Nat Immunol* 4:835–842.
27. Hu C-M, Jang S-Y, Fanzo J-C, Pernis AB (2002) Modulation of T cell cytokine production by interferon regulatory factor-4. *J Biol Chem* 277:49238–49246.
28. Gupta S, Jiang M, Pernis A-B (1999) IFN-α activates Stat6 and leads to the formation of Stat2:Stat6 complexes in B cells. *J Immunol* 163:3834–3841.
29. Nagulapalli S, Atchison M-L (1998) Transcription factor Pip can enhance DNA binding by E47, leading to transcriptional synergy involving multiple protein domains. *Mol Cell Biol* 18:4639–4650.
30. Yamagata T, *et al.* (1996) A novel interferon regulatory factor family transcription factor, ICSAT/Pip/LSIRF, that negatively regulates the activity of interferon-regulated genes. *Mol Cell Biol* 16:1283–1294.
31. Yoshida K, *et al.* (2005) Active repression of IFN regulatory factor-1-mediated transactivation by IFN regulatory factor-4. *Int Immunol* 17:1463–1471.
32. Li-Weber M, Eder A, Krafft-Czepa H, Krammer P-H (1992) T cell-specific negative regulation of transcription of the human cytokine IL-4. *J Immunol* 148:1913–1918.
33. Elser B, *et al.* (2002) IFN-γ represses IL-4 expression via IRF-1 and IRF-2. *Immunity* 17:703–712.
34. Constant S, Pfeiffer C, Woodard A, Pasqualini T, Bottomly K (1995) Extent of T cell receptor ligation can determine the functional differentiation of naïve $CD4^+$ T cells. *J Exp Med* 182:1591–1596.
35. Kubo M, *et al.* (1997) T cell subset-specific expression of the IL-4 gene is regulated by a silencer element and STAT6. *EMBO J* 16:4007–4020.
36. Ozato K, Tailor P, Kubota T (2007) The interferon regulatory factor family in host defense: Mechanism of action. *J Biol Chem* 282:20065–20069.
37. Ishiwata K, Nakao H, Nakamura-Uchiyama F, Nawa Y (2002) Immune-mediated damage is not essential for the expulsion of. *Nippostrongyrus brasiliensis* adult worms from the small intestine of mice. *Parasite Immunol* 24:381–386.

Allele-Selective Effect of PA28 in MHC Class I Antigen Processing[1]

Taketoshi Yamano,[2]* Hidetoshi Sugahara,[2]* Shusaku Mizukami,* Shigeo Murata,[†] Tomoki Chiba,[‡] Keiji Tanaka,[§] Katsuyuki Yui,[¶] and Heiichiro Udono[3]*

PA28 is an IFN-γ-inducible proteasome activator and its genetic ablation causes complete loss of processing of certain Ags, but not all of them. The reason why this occurs and how PA28 influences the formation of peptide repertoires for MHC class I molecules remains unknown. In this study, we show the allele-specific role of PA28 in Ag processing. Retrovirus-transduced overexpression of PA28α decreased expression of K^d (D^d) while it increased K^b and L^d on the cell surface. By contrast, overexpression of PA28αΔC5, a mutant carrying a deletion of its five C-terminal residues and capable of attenuating the activity of endogenous PA28, produced the opposite effect on expression of those MHC class I molecules. Moreover, knockdown of both PA28α and β by small-interfering RNA profoundly augmented expression of K^d and D^d, but not of L^d, on the cell surface. Finally, we found that PA28-associated proteasome preferentially digested within epitopic sequences of K^d, although correct C-terminal flankings were removed, which in turn hampered production of K^d ligands. Our results indicate that whereas PA28 negatively influences processing of K^d (D^d) ligands, thereby, down-regulating Ag presentation by those MHC class I molecules, it also efficiently produces K^b (L^d) epitopes, leading to up-regulation of the MHC molecules. *The Journal of Immunology*, **2008, 181: 1655–1664.**

Major histocompatibility complex class I ligands are produced mainly by proteasomes (1–3). The proteasome activator PA28 (α and β), which is strongly induced by the major immunomodulatory cytokine IFN-γ (1, 4), has been implicated in the regulation of MHC class I Ag processing (5). PA28 accelerates the production of MHC class I ligands from longer precursor peptides by the 20S proteasome in vitro (6). The C-terminal flanking region is critical for efficient production of the T cell epitope (7). It is possible that PA28 activates the 20S proteasome by opening its α-ring (8) that is usually closed and through which substrates can pass into the core catalytic portion. In vivo analysis has also shown that the processing of several, but not all, Ags is stimulated by overexpression of PA28α and PA28β (9). Likewise, the lack of PA28 impairs the ability to process a melanoma Ag TRP2-derived peptide, but does not apparently result in a deficient processing of other Ags such as OVA (10, 11). This indicates that PA28α/β is not a prerequisite for Ag presentation in general, but plays an essential role for the processing of certain Ags. So far, the reason why PA28 is crucial in the processing of certain Ags remains unknown.

IFN-γ stimulation increases expression of the "homo-PA28 proteasome" and the "hybrid proteasome" (12). The former proteasome is a complex where PA28 is attached to both ends of the central 20S proteasome and the latter comprises the 20S proteasome flanked by PA28 on one side and a 19S cap (alias regulatory particle RP or PA700) on the other, functioning as a new ATP-dependent protease, similar to 26S proteasomes, which have a 19S cap on both sides (13). It has been suggested that hybrid proteasomes play a major role in IFN-γ-induced peptide supply for MHC class I molecules, because they can directly process ubiquitylated proteins into MHC class I ligands or into the shortest precursor peptide (14). Indeed, PA28 deficiency suppressed up-regulation of cell surface MHC class I molecules by IFN-γ, even though immunoproteasomes could be induced (10). Thus, PA28, possibly as a hybrid proteasome, is a prerequisite for IFN-γ-induced enhancement of MHC class I expression. Cascio et al. (14) have shown that the peptide repertoire produced in vitro by a hybrid proteasome from insulin growth factor 1 protein was very different from that produced by the 26S proteasome. Considering the essential role of PA28 in IFN-γ-induced enhancement of MHC class I, it is possible that the repertoire of MHC class I ligands changes in response to IFN-γ; however, the PA28-induced peptide repertoire in vivo has not yet been studied and neither has the role of allelic polymorphism on the activity of PA28.

We noticed that expression levels of cell surface K^d and D^d, but not L^d, in BALB/c PA28$\alpha^{-/-}\beta^{-/-}$ cells were slightly higher than those measured on wild-type cells. Knocking down both PA28α and β by small-interfering RNA (siRNA)[4] revealed that K^d and D^d, but not L^d, molecules were extremely up-regulated on the cell

*Laboratory for Immunochaperones, Research Center for Allergy and Immunology, RIKEN Yokohama Institute, Tsurumi, Yokohama, Japan; †Laboratory of Protein Metabolism, Graduate School of Pharmaceutical Sciences, the University of Tokyo, Hongo, Bunkyo-ku, Tokyo, Japan; ‡Graduate School of Life and Environmental Sciences, University of Tsukuba, Tennodai, Tsukuba City, Ibaraki, Japan; §Laboratory of Frontier Science, Tokyo Metropolitan Institute of Medical Science, Honkomagome, Bunkyo-ku, Tokyo, Japan; and ¶Division of Immunology, Department of Molecular Microbiology and Immunology, Graduate School of Biomedical Sciences, Nagasaki University, Sakamoto, Nagasaki, Japan

Received for publication April 23, 2008. Accepted for publication May 14, 2008.

The costs of publication of this article were defrayed in part by the payment of page charges. This article must therefore be hereby marked *advertisement* in accordance with 18 U.S.C. Section 1734 solely to indicate this fact.

[1] This work was supported by a Grant-in-Aid for Scientific Research on Priority Areas from the Ministry of Education, Science, Sports and Culture, Japan.

[2] T.Y. and H.S. contributed equally to this work.

[3] Address correspondence and reprint requests to Dr. Heiichiro Udono, Laboratory for Immunochaperones, Research Center for Allergy and Immunology, RIKEN Yokohama Institute, Tsurumi, Yokohama 230-0045, Japan. E-mail address: udonoh@rcai.riken.jp

[4] Abbreviations used in this paper: siRNA, small-interfering RNA; LC, liquid chromatography; MS, mass spectrometry; VSV, vesicular stomatitis virus; Mϕ, macrophage; MCMV, murine CMV; CSP, circumsporozoite protein; NP, nucleoprotein.

surface. To clarify the role of PA28, we devised a PA28α mutant lacking the five C-terminal residues, designated as PA28αΔC5 and capable of competing with the endogenous PA28. Using this mutant PA28αΔC5 together with knocking down PA28 by siRNA and retrovirus-transduced overexpression of PA28α, we examined the role of PA28 on the cell surface expressions of various MHC molecules. Furthermore, we performed digestion assays with the 20S proteasome mixed with recombinant (r)PA28α (or PA28αΔC5) plus PA28β for several synthetic peptides harboring K^b or K^d ligands, and liquid chromatography/mass spectrometry (LC/MS) analysis revealed that whereas the homo-PA28 proteasome is prone to digest within sequences of K^d ligands even with removing correct C-terminal flanking, it was partly able to produce K^b ligands. Our results indicate that the effect of PA28 in Ag processing, be it positive or negative, is allele specific.

Materials and Methods

Cells and cell culture

RLδ1 is a BALB/c mouse T cell leukemia. EL4 is a methylcholanthrene-induced C57BL/6 mouse thymoma. E.G7 is an OVA cDNA-transfected EL4 cell line (15). $PA28\alpha^{-/-}\beta^{-/-}$ tumor cells is a methylcholanthrene-induced BALB/c fibrosarcoma. CTLs specific for each peptide were generated and maintained as described previously (16). E.G7 was cultured in RPMI 1640 supplemented with 10% FCS (Invitrogen), 1 mM sodium pyruvate, 0.1 mM nonessential amino acids, 20 mM L-glutamic acid, 5×10^{-5}M 2-ME, and penicillin-streptomycin supplemented with 400 μg/ml G418. Cells transfected with a retroviral gene (pMSCVpuro encoding murine PA28α, PA28αΔC5) were selected and maintained with 2 μg/ml puromycin.

Abs, peptides, and reagents

Rabbit polyclonal anti-histidine tag was obtained from MBL. Mouse monoclonal anti-20Sα2, Rpt1. PA28β were obtained from BIOMOL. mAb to PA28α was produced from a hybridoma clone 1G11 in our laboratory. Rabbit polyclonal anti-actin Ab was obtained from Sigma-Aldrich. Mouse monoclonal anti-K^b (AF6-88.5, IgG2a, biotin-conjugated) and D^d (34-5-8S, IgG2a, biotin-conjugated) were obtained from BD Pharmingen. Mouse monoclonal anti-K^d (31-3-4, IgM), anti-L^d (30-5-7, IgG2a) were purified from ascitic fluid. These Abs recognize peptide-bound folded MHC class I molecules. 25D1.16 mAb specific for $OVA_{257-264}$-K^b was provided by Dr. R. Germain (17). Abs specific to heat shock protein 90α were purchased from Stressgen.

The substrate suc-LLVY-amc was obtained from the Peptide Institute. The peptides $OVA_{248-269}$ (EVSGLEQLESIINFEKLTEWTS: underlined residues represent the K^b-restricted epitope), $OVA_{257-269}$ (SIINFEKLTEWTS: K^b), $OVA_{248-264}$ (EVSGLEQLESIINFEKL: K^b), $OVA_{257-264}$ (SIINFEKL: K^b), $TRP2_{181-193}$ (VYDFFVWLHYYSV; K^b), $TRP2_{181-188}$ (VYDFFVWL: K^b) (18), circumsporozoite protein $(CSP)_{281-289}$ (SYVPSAEQI: K^d), and pRL1a (IPGLPLSL; L^d) (19) were purchased from Sawady Technology. For LC/MS analysis, $OVA_{252-269}$, $TRP2_{181-193}$, vesicular stomatitis virus (VSV) NP_{47-66}, HSV glycoprotein $B_{493-512}$, Tum-$P198_{814-828}$, *Listeria monocytogenes* $p60_{212-231}$, Influenza A $HA_{513-532}$, and *Plasmodium yoelii* $CSP_{278-295}$ peptides (with 90% purity) were purchased from Scrum. The sequences of those peptides are indicated in Figs. 6 and 7. As $TRP2_{181-193}$ peptide contains a cysteine residue (Cys^{179}) in its N-terminal flanking, we used only C-terminally extended peptide. Also, Tum-$P198_{14-28}$ peptide has an uncertain amino acid in its N-terminal flanking (XM_214370; HEVGXKYQAVTATLEEKRKE); we used only C-terminally extended peptide. ATP was purchased from Sigma-Aldrich.

Recombinant proteins and plasmids

Purification of murine PA28α was described previously (10). cDNA of murine PA28β was amplified by RT-PCR from the mRNA of EL4 cells and cloned into the pQE31 expression vector (Qiagen) (5′*Sac*I and 3′*Kpn*I), which incorporates a 6x His tag at the N terminus of the protein. Primers for amplification used were: forward, ATGAGCTCCATGGCCA AGCCTTGTG, and reverse, ATGGTACCTCAGTACATCGATGGC TTTT. A series of reverse primers in which the 3′ codon was serially deleted while the 5′ codon was elongated and was used to produce the PA28αΔC1 to PA28αΔC9 deletion mutants (5′*Bam*HI and 3′*Kpn*I). Protein expression was induced by 1 mM isopropyl-β-D-thiogalactoside, and purified with Ni-NTA as described previously (10). Murine PA28α and PA28αΔC5 were also cloned into sites of 5′*Xho*I and 3′*Hpa*I of pMSCV-puro (Takara Bio).

Loading of peptides and proteins, and Ag-presentation assay

rPA28α and its deletion mutants (100 μg) were osmotically loaded into 2×10^6 EL4 cells or LPS blasts with or without synthetic peptides (4 nmol) as described previously (10). The cells were used for CTL assay as described previously (10).

Electrophoresis and peptidase assay

For preparation for cell lysates, EL4 or $PA28\alpha^{-/-}\beta^{-/-}$ cells were lysed with 26S buffer (25 mM Tris-HCl (pH 7.5), 250 mM sucrose, 1 mM DTT, 1 mM PMSF) containing 1% Nonidet P-40 for 30 min on ice, and centrifuged. The supernatants were obtained for electrophoresis. Native PAGE was performed with a 3–10% gradient gel (Wako Pure Chemical). SDS-PAGE was performed using a 5–20% gradient gel. The in-gel hydrolysis assay was performed as described previously (20). Peptidase activity of the proteasome after separation by native PAGE was measured using suc-LLVY-amc (chymotrypsin-like activity). After electrophoresis, the gels were incubated with the substrates (0.1 mM) at 37°C for 10 min. Proteasome bands were then visualized by exposure of the gel to UV light at 360 nm and detected with a 460-nm filter.

Flow cytometry

Cells were suspended in FACS buffer (PBS, 1% FCS, and 0.02% azide) with specific primary Ab and incubated for 30 min at 4°C. They were then washed twice and stained with a second Ab, FITC-conjugated rabbit anti-mouse IgG (H+L), or avidin-conjugated FITC (Jackson ImmunoResearch Laboratories). Flow cytometric analysis was performed on a FACScan (BD Biosciences), and the data were analyzed by CellQuest software (BD Biosciences). The same experiments were also performed with cells treated with 1 ng/ml IFN-γ (R&D Systems) for 48 h. The acid-wash recovery assay was performed as described previously (10).

Small-interfering RNA

Target sequences for PA28α and PA28β were AAGCCAAGGTGGAT GTGTT and AGCGAGCAAGGCCAGAAGC, respectively. Oligonucleotides were cloned into piGENE PUR hU6 plasmid vector (Toyobo). A total of 1×10^6 cells were transfected with the plasmids (2 μg) encoding siRNA by using the Nucleofector device (Amaxa Biosystems).

Purification of the 20S proteasome and its use for peptide digestion assay with LC/MS

Normal mouse livers (10 ml) were homogenized in buffer A (25 mM Tris-HCl (pH 7.5), 1 mM DTT, 0.25 M sucrose, 1 mM PMSF), and centrifuged at 10,000 × *g* for 20 min. The supernatant was further centrifuged at 100,000 × *g* for 1 h, and then, the resulting supernatant was resolved into AKTA FPLC connected with a RESOURCE Q column (Amersham Biosciences) equilibrated with buffer A, and eluted with 0–1 M NaCl gradient at 4 ml/minute for 30 min and collected at 1 ml/fraction/minute. The active fractions (Fr. 7–15) against suc-LLVY-amc with 0.02% SDS were mixed and concentrated with a Centrifugal Filter Device (Ultrafree-0.5; Millipore) and loaded on a heparin column (HiTrap Heparin HP; Amersham Biosciences), followed by elution with 0–1 M NaCl gradient at 2 ml/min for 20 min. The active fractions against suc-LLVY-amc were eluted with <240 mM NaCl, and were further subjected to a hydrophobic column (RESOURCE PHE for HIC; Amersham Biosciences) equilibrated with buffer B (10 mM potassium phosphate (pH 7.5), 1 mM DTT, 0.25 M sucrose) and eluted with 10–500 mM potassium phosphate. The active fractions were collected and concentrated (and washed) by a centrifugal filter device with buffer A. The purified material was prepared at 20 μg/ml with buffer A and used for peptide digestion assay. Synthetic peptide with 90% purity (1 μg) was incubated with 50 ng of 20S proteasome with or without indicated doses of recombinant PA28α, PA28(αΔC5), and PA28β in a 20 μl total volume for 3 h, and 40 μl of 0.2% trifluoroacetic acid was added. After mild pipetting, the sample was kept on ice for 30 min and then applied onto a LC/MS system with electrospray ionization.

For LC/MS, an Alliance 2695 Separation Module attached to an Atlantis dC18 column (Waters) HPLC, online connected to MICROMASS ZQ (Waters), was used. The buffer A and B for HPLC was 0.1% formic acid/water and 0.08 formic acid/water plus 80% acetonitrile, respectively. The acetonitrile gradient was performed from 0 to 80% buffer B for 30 min. Scans were acquired every 1.5 s over a mass range m/z 400 to 1500.

MassLynx and BioLynx protein software were used for data analysis. To monitor hydrolysis activity for suc-LLVY-amc, the 20S proteasome

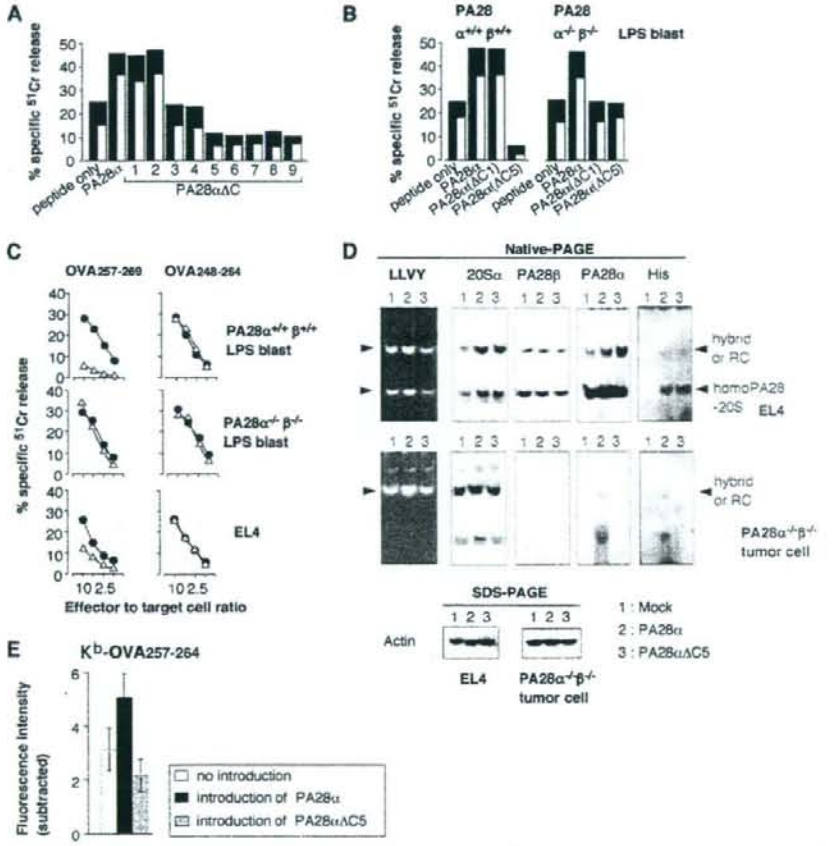

FIGURE 1. Effects of PA28α deletion mutants capable of interfering with PA28 action in Ag processing. *A*. A series of rPA28α deletion mutants ranging from C-terminal residues 1–9 (designated ΔC1 to ΔC9) were osmotically co-introduced with $OVA_{248-269}$ (4 nM) into EL4 cells. The cells were used as target cells in a ^{51}Cr-release assay (E:T ratio 10, ■; E:T ratio 5, □). *B*, PA28α deletion mutants affected Ag processing of PA28$\alpha^{+/+}\beta^{+/+}$ cells but not PA28$\alpha^{-/-}\beta^{-/-}$ cells. Intact PA28α, PA28αΔC1, and PA28αΔC5 were co-introduced with $OVA_{248-269}$ (4 nM) into PA28$\alpha^{+/+}\beta^{+/+}$ or PA28$\alpha^{-/-}\beta^{-/-}$ LPS blasts. The cells were used as target cells in the ^{51}Cr-release assay, as shown in *A*. *C*, Ag processing of COOH- but not NH_2-terminally extended precursor peptides was decreased by PA28αΔC5 in PA28$\alpha^{+/+}\beta^{+/+}$ cells. $OVA_{257-269}$ and $OVA_{248-264}$ (4 nM each) were introduced with (△) or without (●) PA28αΔC5 into EL4 and LPS blasts. The cells were used as target cells in the ^{51}Cr-release assay. *D*. PA28αΔC5 associates with the homo-PA28 proteasome as well as with the hybrid proteasomes. Either PA28α or PA28αΔC5 was osmotically introduced into EL4 (*upper panel*) or PA28$\alpha^{-/-}\beta^{-/-}$ cells (*lower panel*). Two hours later, cell extracts were separated by native PAGE and chymotrypsin-like activity was examined using suc-LLVY-amc. In addition, the native PAGE gels were subjected to Western blotting with specific Abs to polyhistidine, 20Sα2, PA28α, and PA28β. Quantities of loaded proteins were checked by anti-actin Ab (SDS-PAGE). *E*, Intact PA28α and PA28αΔC5 were co-introduced with $OVA_{248-269}$ (4 nM) into EL4 cells. Four hours later, after introduction, the cell surface K^b-$OVA_{257-264}$ complex was examined with 25D1.16 mAb.

(50 ng), mixed with indicated doses of recombinant PA28α, PA28(αΔC5), and PA28β in a total volume of 100 μl, was subjected onto a MultiDetection Microplate Reader, POWERSCAN HT (Dainippon Pharmaceutical).

Results

PA28α deletion mutants capable of interfering with the activity of PA28 in Ag processing

Initially, we tried to obtain PA28α variants that could compete with the action of endogenous PA28 in terms of Ag processing. Because the C-terminal amino acid residues of PA28α are required for binding to the 20S proteasome (21, 22), we examined how various deletion mutants of PA28α influence Ag processing. To this end, we expressed rPA28α mutants whose residues were serially deleted, ranging from 1 to 9 aa at the C terminus, termed PA28αΔC1 to PA28αΔC9, respectively, in *Escherichia coli*, and purified them to near homogeneity. These mutants were osmotically loaded with $OVA_{248-269}$, a precursor polypeptide harboring the CTL epitope $OVA_{257-264}$ of OVA, into EL4 cells ($H\text{-}2^b$), and the cytolysis of the loaded cells by CTLs specific for $OVA_{257-264}$ was monitored. There was still enhanced cytolytic activity with the PA28α mutants carrying deletions of one or two C-terminal residues, similar to wild-type PA28α (Fig. 1*A*). However, no significant enhancement was observed when 3- or 4-aa deletion mutants of PA28α were used. Interestingly, PA28α mutants lacking five to nine residues from the C terminus markedly inhibited the Ag processing. These effects, i.e., enhancement by PA28αΔC1 and inhibition by PA28αΔC5 of the OVA epitope processing, were also observed in C57BL/6 LPS blasts (Fig. 1*B*). Importantly, however, both mutants did not have any influence on Ag processing by LPS blasts derived from PA28$\alpha^{-/-}/\beta^{-/-}$ mice (Fig. 3*B*), indicating that these PA28α variants exert their effects through their association with endogenous PA28α and/or PA28β.

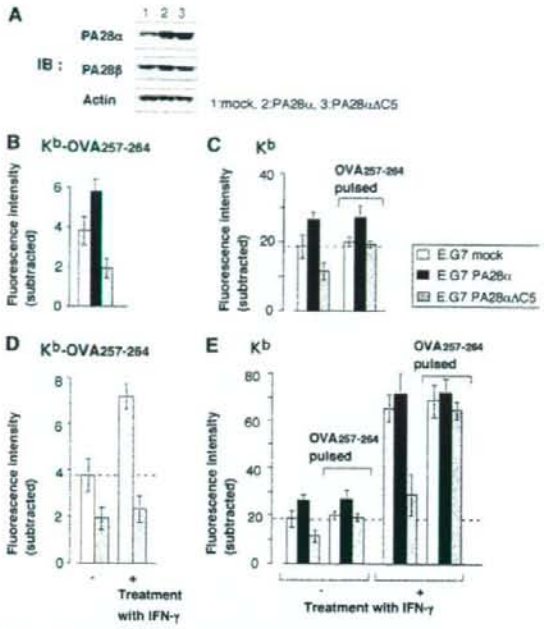

FIGURE 2. PA28 positively influences cell surface expression of K^b-$OVA_{257-264}$ complex and total K^b molecules. *A*, Levels of expressed proteins. The amount of PA28α and PA28αΔC5 in total cell extracts of E.G7mock, E.G7(PA28α), and E.G7 (PA28αΔC5) cells was examined by Western blotting using specific Abs. *B*, Cell surface expression of K^b-$OVA_{257-264}$ complex on OVA-expressing E.G7mock (□), E.G7(PA28α) (■), and E.G7(PA28αΔC5) (▨) cells were analyzed by FACS with mAb 25D1.16. *C*, The cell surface expression of K^b molecules on three transfectants was analyzed by FACS. $OVA_{257-264}$ (10^{-5} M) was also pulsed on cells for 12 h before analysis. *D*, E.G7mock and E.G7(PA28αΔC5) cells treated with or without IFN-γ (1 ng/ml) were analyzed for the cell surface level of K^b-$OVA_{257-264}$ complex. *E*, The level of total K^b molecules on the transfectants, treated with or without IFN-γ (1 ng/ml), was examined. Results of *B–E* are shown as mean fluorescence subtracted of control fluorescence (staining with only second Ab or FITC-conjugated streptavidin) (mean ± SEM; $n = 3$). The result was a representative of three independent experiments.

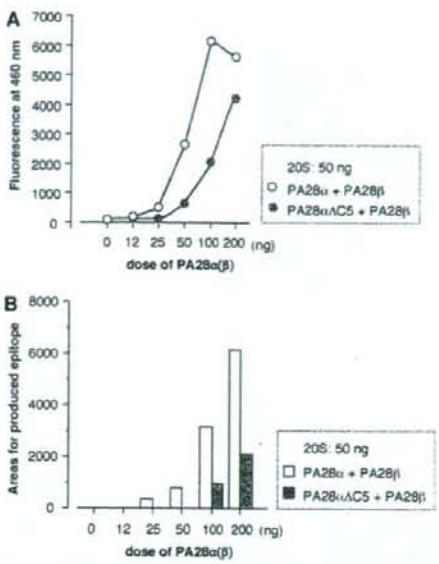

FIGURE 3. Less efficient activity of PA28αΔC5 in hydrolysis of suc-LLVY-amc and production of $TRP2_{181-188}$ from the C-terminally longer precursor. *A*, The 20S proteasome (50 ng) purified from normal mouse liver was mixed with indicated doses of recombinant PA28α, PA28αΔC5, and PA28β in a final 100 μl volume containing 0.1 mM suc-LLVY-amc and was then subjected onto a MultiDetection Microplate Reader to detect fluorescence activity. *B*, The same preparation as in *A*, but total volume was 20 μl, was added with synthetic peptide $TRP2_{181-193}$ (1 μg) and incubated for 3 h at 37°C. The produced K^b epitope, $TRP2_{181-188}$, was detected by LC/MS analysis. The quantity of detected epitope was indicated as areas of [M+H] m/z. The result was a representative of three independent experiments.

We reported previously that PA28 promoted the processing of extended precursor peptides harboring the $OVA_{257-264}$ epitope sequence that had been extended on their C terminus, but not if they had been extended at their only N terminus (10). Therefore, the two peptides, $OVA_{257-269}$ (C-terminal extension) and $OVA_{248-264}$ (N-terminal extension), were loaded into EL4 or LPS blasts from $PA28\alpha^{+/+}/\beta^{+/+}$ and $PA28\alpha^{-/-}/\beta^{-/-}$ mice with or without PA28αΔC5. As shown in Fig. 1*C*, the inhibitory effect of PA28αΔC5 on cytolysis was observed in EL4 and the wild-type LPS blasts loaded with $OVA_{257-269}$ but not $OVA_{248-264}$. In contrast, PA28αΔC5 showed no effect on $PA28\alpha^{-/-}/\beta^{-/-}$ LPS blasts (Fig. 1*C*). These results strongly indicate that PA28αΔC5 blocks the C-terminal processing of the precursor peptide $OVA_{257-269}$ by using endogenous PA28.

To understand the activity of PA28αΔC5, we subsequently examined its association with the 20S proteasome in the cells. PA28αΔC5 or PA28α were loaded into EL4 cells or $PA28\alpha^{-/-}\beta^{-/-}$ cells, and 2 h later, the cell lysates were subjected to native PAGE to analyze enzyme activities and structures of the proteasome. PA28α increased the chymotrypsin-like activity of the hybrid as well as of the homo-PA28 proteasome, whereas PA28αΔC5 slightly decreased the activity (Fig. 1*D*, *left end panel*). Both PA28α and PA28αΔC5 associated with the hybrid as well as with the homo-PA28 proteasome in EL4 cells, but only PA28α associated with these proteasomes in $PA28\alpha^{-/-}\beta^{-/-}$ cells as judged by Western blotting with anti-histidine Ab and other Abs indicated in Fig. 1*D*. PA28αΔC5 should not be able to bind to the 20S proteasome because several C-terminal residues of PA28α are critical for binding. Deletion of only one residue at the C terminus of PA28α prevents its association with the α-ring of the 20S proteasome, as previously indicated (22). Exogenously introduced PA28α does not need endogenous PA28 to bind to the 20S proteasome, i.e., the homopolymeric PA28α complex can associate with the 20S proteasome in vivo. This is consistent with previous findings showing that it functions as an activator in vitro (5). We also confirmed that osmotic cointroduction of $OVA_{248-269}$ with PA28α but not PA28αΔC5 into EL4 cells increased the cell surface K^b-$OVA_{257-264}$ complex, compared with $OVA_{248-269}$ alone (Fig. 1*E*).

PA28 augments the cell surface expression of the K^b-$OVA_{257-264}$ complex and of total K^b

Subsequently, we prepared stable lines of E.G7 cells expressing a full-length OVA gene transfected with PA28α, PA28αΔC5, and mock plasmid (pMSCV empty vector), designated E.G7(PA28α), E.G7(PA28αΔC5), and E.G7mock, respectively. Western blot analysis revealed that E.G7(PA28α) and E.G7(PA28αΔC5) produced 2- and 3-fold more PA28α and PA28αΔC5, respectively, than endogenous PA28α measured in E.G7mock cells (Fig. 2*A*).

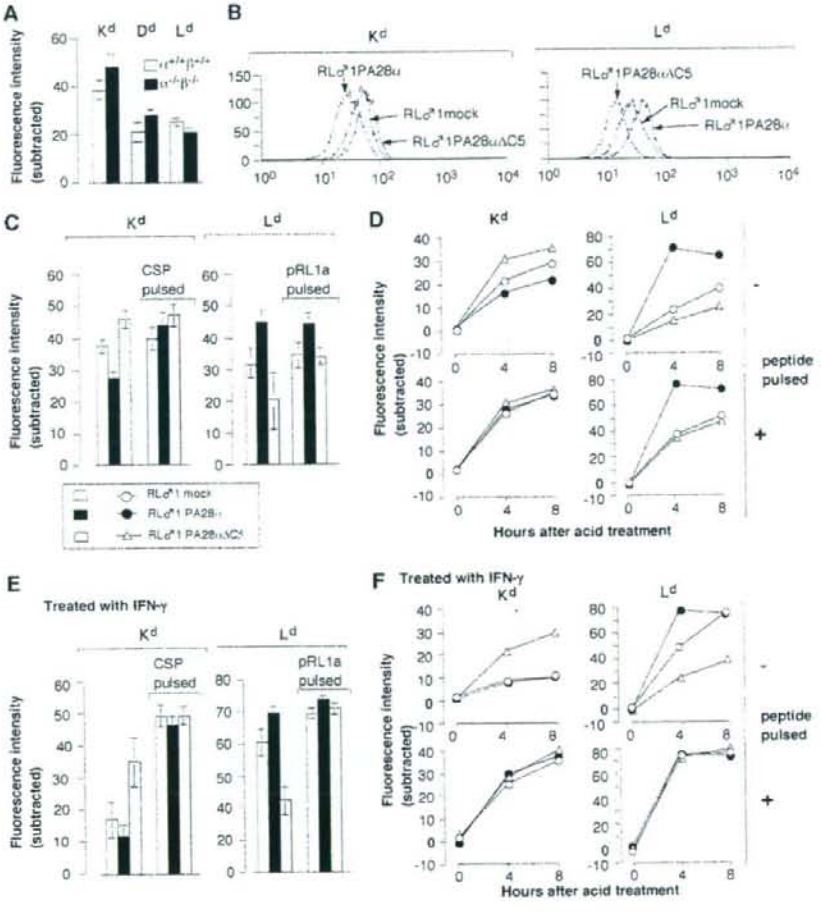

FIGURE 4. PA28 negatively influences cell surface expression of K^d, D^d, but not L^d. *A*, Peritoneal Mϕ derived from BALB/c PA28$\alpha^{+/+}$ $\beta^{+/+}$ and PA28$\alpha^{-/-}\beta^{-/-}$ mice were analyzed for expression of K^d, D^d, and L^d. *B*, Cell surface expression levels of K^d and L^d on RLδ1(PA28α), RLδ1(PA28$\alpha\Delta$C5), and RLδ mock cells are shown as histograms. Gray shadows indicate staining with only avidin-FITC or second Abs conjugated with FITC. *C*, Data for *B* are shown as bar graphs. MHC class I-specific ligands ($CSP_{281-289}$ for K^d, pRL1a for L^d; 10^{-5} M) were also pulsed on those transfectants for 12 h before analysis. *D*, Acid-wash recovery of K^d and L^d molecules. RLδ1(PA28α), RLδ1(PA28$\alpha\Delta$C5), and RLδ mock cells were treated with acid (pH 3.0), and incubated with or without specific ligands for 8 h to examine the recovery of K^d and L^d molecules. The mean fluorescence was plotted. *E*, IFN-γ (1 ng/ml, 48 h)-treated RLδ1 (PA28α), RLδ1(PA28$\alpha\Delta$C5), and RLδ mock cells were analyzed as in *C*. *F*, Acid-wash recovery assay with IFN-γ-treated (1 ng/ml, 48 h) RLδ1 (PA28α), RLδ1(PA28$\alpha\Delta$C5), and RLδ mock cells were performed as in *D* (mean ± SEM; $n = 3$). The result was a representative of three independent experiments.

We also examined the amount of cell surface of K^b-$OVA_{257-264}$ and total K^b for each transfectant cultured with or without IFN-γ. In the absence of IFN-γ, PA28α up-regulated the K^b-$OVA_{257-264}$ complex and total K^b but PA28αΔC5 markedly suppressed expression of both K^b-$OVA_{257-264}$ and total K^b (Fig. 2, *B* and *D*). The inhibitory effect by PA28αΔC5 was still visible after 3 days of culture with IFN-γ (data not shown). The down-regulation of K^b expression was completely restored by a pulse of E.G7 (PA28αΔC5) with $OVA_{257-264}$ (Fig. 2, *C* and *E*), indicating that the diminished supply of endogenous peptides was responsible for the down-regulated expression. Expression of D^b by those transfectants was almost the same as that of K^b (data not shown).

PA28αΔC5 was less efficient in production of $TRP2_{181-188}$ from C-terminally longer precursors, compared with intact PA28α

PA28α enhanced the expression of K^b-$OVA_{257-264}$ and total K^b, in contrast, PA28αΔC5 suppressed those, as shown in Fig. 2. Therefore, we investigated in the vitro effect of PA28α plus PA28β and PA28αΔC5 plus PA28β together with the 20S proteasome on production of $TRP2_{181-188}$ from C-terminally longer precursors whose processing was previously shown to be dependent on PA28 (13). The 20S proteasome (50 ng) purified from mouse liver was mixed with graded doses of recombinant PA28α (or PA28αΔC5) and PA28β in a volume of 20 μl, and then added with 1 μg of $TRP2_{181-193}$, followed by incubation for 3 h at 37°C. A total of 40 μl 0.2% trifluoroacetic acid was added to the mixture and a 10 μl total volume was injected into LC/MS to detect exact K^b-epitope $TRP2_{181-188}$. Simultaneously, hydrolysis activity for suc-LLVY-amc was examined. The results showed that both hydrolysis activity and production of $TRP2_{181-188}$ by PA28αΔC5 were significantly lower than those by PA28α (Fig. 3).

PA28 attenuates cell surface expression of K^d and D^d but not L^d

We next examined the effects of PA28α and PA28αΔC5 on the expression of MHC class I molecules other than K^b and D^b. The cell surface expression of K^d and D^d on peritoneal macrophages (Mϕ) of BALB/c PA28$\alpha^{-/-}\beta^{-/-}$ mice was significantly higher than on Mϕ of wild-type mice, whereas, in contrast, L^d expression was slightly lower in Mϕ of PA28$\alpha^{-/-}\beta^{-/-}$ (Fig. 4*A*). To assess directly the effects of PA28α and PA28αΔC5, we established BALB/c RLδ1(H-2^d) expressing PA28α, PA28αΔC5, and mock plasmid, designated RLδ1 (PA28α), RLδ1 (PA28αΔC5), and RLδ1mock, respectively, and cell surface MHC class I molecules of those transfectants were examined. Surprisingly, expression of K^d was down-regulated but that of L^d was enhanced by PA28α, whereas PA28αΔC5 induced the opposite effects (Fig. 4*B*). The expression of K^d was restored to normal level by a pulse with $CSP_{281-289}$ derived from *P. yoelii* (23) (Fig. 4*C*). In an acid-wash recovery assay, PA28α delayed the recovery of K^d, whereas

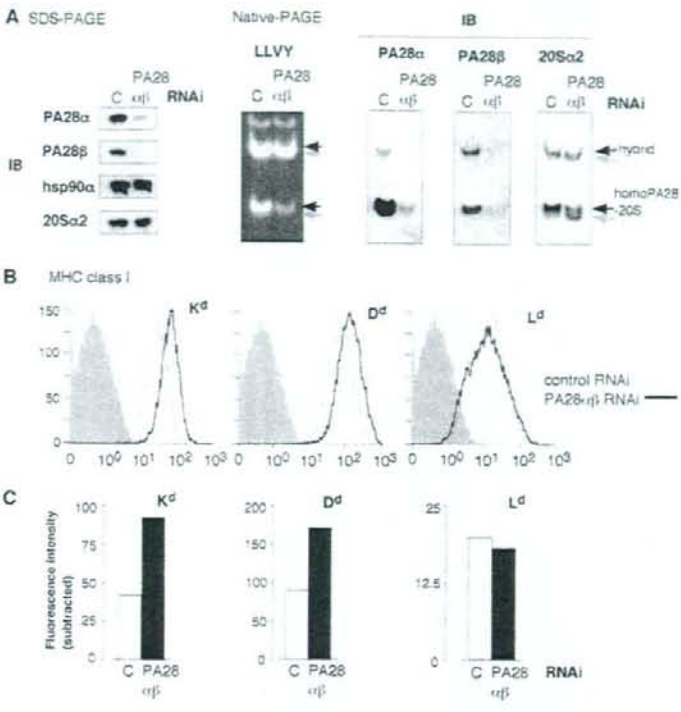

FIGURE 5. Depletion of PA28α and β by siRNA augments cell surface expression of K^d, D^d, but not L^d. *A*, MEF/3T3 cells were transfected with siRNA against PA28α and β, or with a vector not encoding siRNA. After 48 h, expressed proteins were examined by SDS-PAGE followed by Western blotting with the indicated Abs. The peptidase activity for suc-LLVY-amc and the structure of the proteasome were examined. *B*, Expression of MHC class I K^d, D^d, L^d of MEF/3T3 cells in *A* was examined by FACS analysis. *C*, Mean fluorescence intensities of K^d, D^d, and L^d in *B* are shown as bar graphs.

PA28αΔC5 accelerated the recovery (Fig. 4*D*). A pulse with $CSP_{281-289}$ restored the delayed recovery of K^d (Fig. 4*D*). These results clearly show that PA28α is responsible for the shortage of K^d ligands in the cells. By contrast, expression of L^d was restored by a pulse with an exact L^d epitope, pRL1a (19) (Fig. 4*C*). In acid-wash recovery, PA28α accelerated, whereas PA28αΔC5 delayed, the recovery of L^d (Fig. 4*D*). The delayed recovery of L^d was restored by a pulse with pRL1a (Fig. 4*D*). The results indicate that PA28α stimulates the production of L^d ligands in cells, in contrast to its effect on the production of K^d ligand.

The negative impact of PA28α on K^d expression was further examined in the context of IFN-γ treatment which strongly induces endogenous PA28. IFN-γ treatment appeared to starve endogenous K^d ligands in RL♂1 (PA28α) more than in RL♂1 (PA28αΔC5) because the relative restoration level of K^d by a pulse with the CSP epitope was much larger in RL♂1 (PA28α) (Fig. 4*E*, *left panel*). Exactly the opposite effect was seen for expression of L^d, and IFN-γ-treated RL♂1 (PA28αΔC5) starved L^d ligands relative to RL♂1 (PA28α) (Fig. 4*E*, *right panel*). An acid-wash recovery assay supported the negative effect of PA28 in the recovery of K^d molecules: indeed, PA28αΔC5 helped the rapid recovery of K^d molecules whereas it suppressed the recovery of L^d molecules (Fig. 4*F*).

Next, we knocked down the expression of both PA28α and β of MEF/3T3 by siRNA to confirm the effects of PA28. As shown in Fig. 5*A*, expression of both PA28α and β was specifically repressed (80 ~ 90%) but expression of heat shock protein 90α and the 20Sα2 subunit was not altered, and hydrolysis activity to the substrate suc-LLVY-amc was decreased especially in the homo-PA28 proteasome. Native-PAGE followed by Western blotting with Abs to PA28α, β, and 20Sα2, showed a decrease of the hybrid proteasome as well as the homo-PA28 proteasome but not of the singly capped 26S proteasome (RC) and the probably empty 20S proteasome (C) (Fig. 5*A*). Intriguingly, expression of K^d and D^d but not L^d was enhanced by depletion of PA28α and β (Fig. 7*B*) and those alterations are shown in Fig. 5*C*, which confirms the negative effect of PA28 on the expression of K^d and D^d.

The PA28-20S proteasome improperly processes epitopes of K^d but produces K^b ligands

So far, our results consistently suggest that for the ligands used in this study, PA28 augments the generation of ligands for D^b, K^b, and L^d, while it attenuates the production of K^d and D^d ligands. It is crucial to know the reason why PA28 negatively influences K^d and D^d ligand production. To this end, in the next series of experiments, we investigated whether PA28 has a different influence on in vitro digestion using several precursor peptides. For this, we prepared four K^b, four K^d, and one L^d ligands extending C-terminal (and/N-terminal) flanking regions, although these peptides are not necessarily the relevant or native precursors. We digested them with the 20S proteasome alone or plus recombinant PA28α and PA28β, or plus PA28αΔC5 and PA28β.

We observed exact K^b ligands produced from $OVA_{252-269}$, $TRP2_{181-193}$, HSV 16 glycoprotein $B_{493-512}$, VSV NP_{47-66}, and also observed N-terminal extended L^d precursor peptide from murine CMV $pp89_{163-182}$ (Figs. 6 and 7), although some of these epitopes were also partly digested. The 20S proteasome alone did not produce epitope fragments from $OVA_{252-269}$, $TRP2_{181-193}$, and VSV NP_{47-66}, but in the presence of PA28, exact epitopes were cleaved. An epitope from HSV glycoprotein $B_{493-512}$ was produced by the 20S proteasome alone and the quantity was further enhanced by PA28 (Fig. 7). Thus, in these cases, PA28 positively influenced cleavage of the K^b and L^d epitopes. In contrast, exact K^d ligands or its precursors were not recovered by the same proteasome preparations from *L. monocytogenesis* $p60_{212-231}$, Tum-$P198_{14-28}$, influenza A HA $_{513-532}$, *P. yoelii* $CSP_{278-295}$

Peptide sequences	Fragments	RT	m/z [M+H]	m/z [M+2H]	20S + PA28α+β	20S + PA28αΔC5+β	-
A OVA$_{252-269}$ (K^b)	LEQLE	15.2	631.3	-	51395	40354	N.D.
▼ ▼ ▼	SIINFEKL	21.5	963.5	-	1413	N.D.	N.D.
LEQLE SIINFEKL TEWTS			-	482.6	158220	110529	N.D.
	TEWTS	14.7	623.3	-	8920	5370	N.D.
	SIINFEKL TE	21.3	-	597.3	159878	125436	N.D.
	LEQLE SIINFEKL TE	24.5	-	903.5	7292	4100	N.D.
	SIINFEKL TEWTS	24.0	-	784.4	7045	5404	N.D.
B TRP2$_{181-193}$ (K^b)	VYDFFVWL	30.7	1088.8	-	2002	758	N.D.
▼ ▼			-	544.8	7297	1476	N.D.
VYDFFVWL HYYSV	HYYSV	14.6	668.3	-	14067	3188	N.D.
	VYDFF	23.8	690.3	-	12497	1645	N.D.
C L. monocytogenesis p60$_{212-231}$ (K^d)	WALSV	22.3	575.3	-	26962	20945	23594
▼ ▼ ▼▼	KYGVSV	14.7	652.4	-	4521	813	333
WASV KYGVSVQDI MSWNNL	QDI MSWNNL	23.4	1120.5	-	1202	792	380
			-	561.3	31045	20278	8679
	QDI MSWN	20.6	893.4	-	7533	1210	N.D.
	QDI MSW	21.9	779.3	-	6098	3484	N.D.
D Tum-P198$_{14-28}$ (K^d)	KYQAVTA	12.3	780.4	-	201538	133012	996
	TL EEKRKE	8.9	1032.6	-	17648	13920	N.D.
			-	517.1	579974	433348	8266
▼▼ ▼ ▼	KYQAV	11.6	608.3	-	39980	24287	1736
KYQAVTATL EEKRKE	TATL EEKRKE	10.1	-	603.0	9229	6990	N.D.
	KYQA	9.3	509.3	-	119784	86127	1762
	EEKRKE	11.2	818.4	-	12351	9715	N.D.
			-	409.7	26243	10053	N.D.
	LMYD	16.2	541.2	-	439493	228988	12928
	M YPHFMPTNL	21.7	1250.6	-	3558	1611	N.D.
E MCMV pp89$_{163-182}$ (L^d)			-	625.8	1137248	416517	18625
▼▼ ▼ ▼ ▼	GPSEKR	11.4	673.4	-	4445	3924	280
LMYDM YPHFMPTNL GPSEKR	DM YPHFMPTNL	22.9	-	683.3	34238	95903	6325
	LMYDM YPHFMPTNL	24.5	-	686.9	29253	29074	18740
	PHFMPTNL GPSEKR	15.7	-	806.0	12580	11080	673
			-	538.0	603028	386735	90538
	PHFMPTNL	19.3	956.8	-	9069	2781	N.D.
			-	478.9	903968	452423	17848
	PTNL	12.9	444.2	-	147380	88920	7105

FIGURE 6. Digesting patterns of precursor peptides harboring K^b, K^d, and L^d ligands by the proteasome. One microgram of each peptide, *A–E*, was incubated with the 20S proteasome (50 ng) mixed with 100 ng each of PA28α plus PA28β, or PA28αΔC5 plus PA28β in 20 μl total volume for 3 h at 37°C. *A*, OVA$_{252-269}$; *B*, TRP2$_{181-193}$; *C*, *L. monocytogenesis* p60$_{212-231}$; *D*, Tum-P198$_{14-28}$; *E*: MCMV pp89$_{163-182}$. The digestion mixture was subjected onto LC/MS analysis to detect peptide fragments. Amino acid sequences, their retention time (RT), and area determined by m/z values of [M+H] and [M+2H] of digested fragments were indicated. Horizontal lines under peptide sequences indicated the recovered fragments after digestion. Quantity of each fragment produced by the 20S proteasome and PA28α and PA28β is visualized as follows: >1,000,000 (thickest black bar), 100,000~999,999 (second thickest black bar), 10,000~99,999 (third thickest black bar), 1,000~9,999 (thinnest black bar). Cleavage points by the proteasome were also indicated by inverted triangles (▼) whose sizes paralleled with obtained quantity (area) of the digested fragments. The exact MHC class I epitope is depicted with bold (and/or underlining). Note that each retention time (RT) of the exact epitope produced by digestion of *A*, *B*, and *E* was precisely the same as that of the synthetic corresponding peptide. None of the exact epitope was observed among the digested materials of *C* and *D*. N.D., Not detected or <100.

(Figs. 6 and 7). Correct C-terminal flanking was not removed from *L. monocytogenesis* p60$_{212-231}$, which resulted in improper processing of the epitope. Even when correct C-terminal flanking was removed from Tum-P198$_{14-28}$, influenza A HA $_{513-532}$, and *P. yoelii* CSP$_{278-295}$, strong digestion within the epitopes occurred in the presence of PA28, which might result in destruction of the epitopes. Importantly, even the 20S proteasome alone efficiently digested within the epitope of influenza A HA$_{513-532}$, but the presence of PA28αΔC5 diminished production of those fragments, while in contrast, intact PA28α augmented those cleavages (Fig. 7). This evidence suggested that PA28αΔC5 could regulate (or suppress) the 20S proteasome-induced overdigestion of particular peptides, while intact PA28α could stimulate it. Although there was a number of reason(s) for the improper processing, this evidence accounted for the reason why PA28 negatively influenced production of K^d ligands by the proteasome.

Almost all fragments or epitopes produced by PA28αΔC5 plus PA28β and the 20S proteasome were lower in quantity than that by PA28α plus PA28β, which was a reasonable outcome because of its undermined enzyme activity, although there were some exceptions. One N-terminal extended a precursor of MCMV pp89$_{163-182}$ (L^d) (Fig. 6) and the exact epitope from HSV glycoprotein B$_{493-512}$ (K^b) (Fig. 7)—both of which were evaluated as areas by [M+2H] were higher in quantity by PA28αΔC5 plus PA28β—and

Peptide sequences	Fragments	RT	m/z [M+H]	m/z [M+2H]	20S + PA28α+β	20S + PA28αΔC5+β	-
A HSV glycoprotein B $_{493-512}$ (K^b)	IKTT SSIEFARL	19.3	-	683.8	16981	8203	1060
RIKTT SSIEFARL QFTYNHI	QFTYNHI	17.4	922.4	-	274	260	315
			-	462.1	66792	58377	39809
	SSIEFARL	19.8	922.5	-	1789	505	562
			-	462.1	112873	345833	42884
	SSIEFA	18.4	653.3	-	184370	89976	2306
	RL QF	16.8	563.3	-	59862	36951	6276
	TYNHI	13.1	647.3	-	1854	604	649
	FARL Q	17.2	634.4	-	7169	6362	1079
	T SSIEF	19.4	583.3	-	15392	8477	677
B VSV NP $_{47-66}$ (K^b)	RGYVYQGL	17.9	-	487.0	52399	26789	N.D.
SLSDL RGYVYQGL KSGNVSI	KSGNVSI	13.0	704.4	-	121896	87264	5997
	SLSDL RGYVYQ	19.8	-	651.2	251815	201636	N.D.
	GL KSGNVSI	15.6	874.5	-	7662	4583	N.D.
			-	438.0	331771	323996	30341
	SLSDL RGYVY	20.5	1172.6	-	58989	27473	N.D.
			-	587.2	4395641	3157001	277816
	QGL KSGNVSI	15.9	1002.6	-	43380	23278	N.D.
			-	502.1	2807918	2097491	192189
	SLSDL RGY	17.5	-	456.0	405458	293147	N.D.
	L KSGNVSI	19.0	817.5	-	7950	6533	N.D.
C Influenza A HA $_{513-532}$ (K^d)	YSTVASSL V	28.8	926.5	-	20766	7933	19223
YQILA IYSTVASSL VLLVSL			-	463.7	50717	13494	35140
	STVASSL VLLVSL	28.6	1288.8	-	7699	793	1588
			-	645.2	61434	22409	43243
	VASSL VLLVSL	27.9	1100.7	-	43331	4331	15351
			-	550.7	404782	240162	307400
	ASSL VLLVSL	26.7	1002.0	-	50407	9682	28899
			-	501.8	18573	3751	6716
	L VLLVSL	26.3	756.6	-	1499339	535959	934015
	L VLL	22.6	457.3	-	369364	167166	38134
	VLLVSL	23.6	643.4	-	89055	104142	237403
	VLLV	20.4	443.2	-	755460	459677	118228
D Plasmodium yoelii CSP $_{278-295}$ (K^d)	NEDSYVQSAE	16.0	1110.9	-	3266	1782	N.D.
NED SYVPSA EQI LEFVKQ	QI LEFVKQ	19.1	-	502.8	305057	254610	16546
	SYVPSAE	15.1	752.3	-	10172	9622	N.D.
	LEFVKQ	16.4	763.4	-	5403	5737	N.D.

FIGURE 7. Digesting patterns of precursor peptides harboring K^b, K^d, and L^d ligands by the proteasome, the same as in Fig. 1, except peptides were digested by the proteasome. *A*, HSV glycoprotein $B_{493-512}$; *B*, VSV NP_{47-66}; *C*, Influenza A $HA_{513-532}$; *D*, *P. yoelii* $CSP_{278-295}$. The exact MHC class I epitope is depicted with bold (and/or underlining). Note that each retention time (RT) of the exact epitope produced by digestion of *A* and *B*, was precisely the same as that of the synthetic corresponding peptides. None of the exact epitope was observed among the digested materials of *C* and *D*. N.D., Not detected or <100.

the reason was unknown. However, we observed no significant difference in cleavage pattern of all peptides used in this study between PA28α plus PA28β and PA28αΔC5 plus PA28β. PA28-20S proteasome-mediated improper processing of K^d ligands tested here might be compromised by PA28αΔC5, which in turn prevents overdigestion of C-terminally elongated precursors. It is noted that the cleavage pattern of all peptides after incubation for 1, 3, and 6 h with the proteasome was nearly comparable, although the longer reaction showed larger quantity of each fragment (data not shown).

Discussion

Ag processing and presentation is crucial for the initiation of the immune response. Over the past decade, there is growing evidence that the proteasome, a large multisubunit protein degradative machinery in eukaryotes, plays an important role as a processing enzyme responsible for the generation of MHC class I ligands (1–3). This processing system is elaborately regulated by various immunomodulatory cytokines. In particular, IFN-γ induces the formation of the immunoproteasomes, in which three IFN-γ-inducible subunits (i.e., β1i, β2i, and β5i) can replace the constitutive catalytic 20S subunits (i.e., β1, β2, and β5) during proteasome biogenesis (24). Furthermore, IFN-γ also induces PA28, producing the homo-PA28-20S proteasome and the hybrid proteasome, which contributes importantly to efficient production of MHC class I ligands (6, 12). Furthermore, it has been shown that the immunoproteasome and the PA28-containing proteasome in concert or independently play a critical role in the generation of the MHC class I ligands (1). However, the molecular mechanisms underlying the correct generation of CTL epitopes by those different types of proteasomes remain a mystery.

In the present study, we tried to clarify the role of the IFN-γ-inducible proteasome activator PA28 in the Ag-processing and -presentation pathway, and surprisingly found different effects of

PA28 on the MHC class I epitope generation depending on the allelic polymorphism. Indeed, whereas PA28 is unable to produce many of K^d ligands and thereby attenuates cell surface expression of those MHC class I molecules, it is able to produce most (if not all) K^b (also L^d) epitopes, leading to up-regulation of the corresponding MHC molecules on the cell surface. Our previous observation that IFN-γ-induced up-regulation of K^b was canceled in PA28-deficient cells (10) is consistent with the present findings and indicate that PA28 plays a prominent role in IFN-γ-stimulated peptide supply. Conversely, knockdown of both PA28α and PA28β by siRNA significantly increased the expression of K^d and D^d (Fig. 5, *B* and *C*), indicating that PA28 negatively influences the presentation of those ligands. Indeed, constitutive expression of K^d and D^d in peritoneal Mϕ from the BALB/c PA28$\alpha^{-/-}\beta^{-/-}$ mouse was slightly higher than on wild-type Mϕ, whereas that of L^d was lower (Fig. 4*A*). Acid-wash recovery of cell surface K^d of RLδ1 cells was accelerated in the presence of PA28αΔC5, especially upon IFN-γ treatment in which endogenous PA28 was extremely induced; in contrast, recovery of L^d was mostly retarded by PA28αΔC5 but accelerated by intact PA28α (Fig. 4*F*). These results clearly support the negative and positive influence of PA28 on the processing of K^d and L^d ligands, respectively.

Why PA28 contributes differently to the MHC class I ligand generation in an allelic polymorphism-dependent fashion is largely unknown. We therefore analyzed a series of synthetic peptides harboring various epitopes whose in vitro digestion was conducted by the PA28-20S proteasome to evaluate from which types of peptides correct epitopes are produced. The PA28-20S proteasome was unable to process any of the K^d ligands tested in this study from their longer precursors, although K^b ligands were efficiently processed by the same proteasome preparation (Figs. 6 and 7). This finding, however, is not in agreement with previous observations that a K^d ligand of JAK1 kinase, SYFPEITHI, was efficiently produced from a longer precursor peptide by the PA28-20S proteasome (6). In fact, we confirmed the enhancing effect of PA28 on processing of this epitope in vivo by osmotically loading the precursor peptides and rPA28α into P815 (H-2^d) cells and also in vitro peptide digestion assay with PA28-20S proteasome (data not shown). The reason for this discrepancy is unknown at present. Nonetheless, considering the clear negative effect of siRNA-mediated knockdown of PA28α and β on K^d (D^d) expression, we emphasize that the majority of those ligands, if not all, are likely to be improperly or inefficiently processed by the PA28-20S proteasome. In vitro production of mouse T cell epitopes from longer precursors by the PA28-20S proteasome was mainly observed in the context of L^d and K^b, although only the JAK1 kinase-derived epitope was K^d restricted as described (6). For example, the mouse leukemia peptide pRL1a (7, 25) and the MCMV pp89-derived peptide (6) were for L^d, and the Moloney murine leukemia virus *gag*-derived peptide (9) and the melanoma Ag TRP2 peptide (10, 11) are K^b ligands. Our current observation that PA28 stimulates the processing of K^b and L^d is consistent with those reports, especially results of in vitro peptide digestion supporting the positive influence of PA28 on the production of K^b ligands by the PA28-20S proteasome (Figs. 6 and 7).

It should be pointed out that production of K^d ligands in vivo was absolutely dependent on the proteasome because acid-wash recovery of K^d as well as L^d was significantly delayed by treatment with the proteasome inhibitor lactacystin (data not shown), suggesting that the 26S proteasome rather than the PA28-20S or another type of proteasome flanked with the newly identified regulatory particle like PA200 (26, 27) and/or the immunoproteasome might be responsible for processing of K^d ligands. To this point, for the processing of *P. yoelii* $CSP_{278-295}$ and Tum-$P198_{14-28}$, we observed that a fraction of the 26S proteasome purified from the liver of the PA28$\alpha^{-/-}\beta^{-/-}$ mouse could exactly produce the K^d epitopes, from the same precursors, although these epitopes were not efficiently produced by the PA28-20S proteasome purified from a wild-type mouse liver (data not shown). The other two K^d ligands used in this study were not processed by the 26S proteasome (data not shown), which might suggest the involvement of the aforementioned different proteasomes or of other so far unidentified molecule(s) in the processing of those peptides. However, the processing mechanisms mediated by the proteasome are intriguing in general, because while it is generally accepted that the immunoproteasome is able to dominantly generate a diverse array of epitopes (1), the processing of some Ags is catalyzed specifically by the standard proteasome (alias constitutive proteasome), but not the immunoproteasome (28). Yet, no one knows the mechanistic reason(s) for those different processing profiles.

Our results clearly demonstrate the allele-specific effect of PA28 on the expression of MHC class I, regardless of the fact that these effects are positive or negative. Pool sequencing of peptides eluted from MHC class I molecules of cells, or large sequencing of individual peptides, would provide more direct information on the effect of PA28 in epitope generation. We could not identify a common reason for the inefficient processing of K^d ligands by the PA28-20S proteasome in this study. However, anchor residues of MHC class I ligands (29) might be, at least in part, involved in the allele-specific effect of PA28. Thus, it is possible that tyrosine anchor residue of K^d ligand is responsible for inefficient processing of many of K^d ligands. We are currently focusing on this issue. Mouse K^d-binding peptides have motif xYxxxxxxL. Because human HLA-A24 ligands also contain the same binding motif, it will be interesting to investigate whether processing of human HLA-A24 ligands is also down-regulated by the PA28 proteasome. Should these findings apply also to Ag processing and MHC class I expression in humans, they would have a great impact on our understanding of the immune system, and have practical implications especially for vaccination strategies in cancer and infectious diseases. Further studies are necessary to fully demonstrate the role of PA28 in allele-specific Ag processing.

Acknowledgments

We are grateful to T. Hiroiwa and C. Kajiwara for preparation of recombinant proteins. We also thank D. Tsubokawa for assistance in proteasome purification and for conducting LC/MS.

Disclosures

The authors have no financial conflict of interest.

References

1. Tanaka, K., and M. Kasahara. 1998. The MHC class I ligand-generating system: roles of immunoproteasomes and the interferon-γ-inducible proteasome activator PA28. *Immunol. Rev.* 163: 161–176.
2. Kloetzel, P. M., and F. Ossendorp. 2004. Proteasome and peptidase function in MHC-class-I-mediated antigen presentation. *Curr. Opin. Immunol.* 16: 76–81.
3. Rock, K. L., I. A. York, T. Saric, and A. L. Goldberg. 2002. Protein degradation and the generation of MHC class I-presented peptides. *Adv. Immunol.* 80: 1–70.
4. Fruh, K., and Y. Yang. 1999. Antigen presentation by MHC class I and its regulation by interferon γ. *Curr. Opin. Immunol.* 11: 76–81.
5. Rechsteiner, M., C. Realini, and V. Ustrell. 2000. The proteasome activator 11 S REG (PA28) and class I antigen presentation. *Biochem. J.* 345(Pt. 1): 1–15.
6. Dick, T. P., T. Ruppert, M. Groettrup, P. M. Kloetzel, L. Kuehn, U. H. Koszinowski, S. Stevanovic, H. Schild, and H. G. Rammensee. 1996. Coordinated dual cleavages induced by the proteasome regulator PA28 lead to dominant MHC ligands. *Cell* 86: 253–262.
7. Shimbara, N., H. Nakajima, N. Tanahashi, K. Ogawa, S. Niwa, A. Uenaka, E. Nakayama, and K. Tanaka. 1997. Double-cleavage production of the CTL epitope by proteasomes and PA28: role of the flanking region. *Genes Cells* 2: 785–800.
8. Whitby, F. G., E. I. Masters, L. Kramer, J. R. Knowlton, Y. Yao, C. C. Wang, and C. P. Hill. 2000. Structural basis for the activation of 20S proteasomes by 11S regulators. *Nature* 408: 115–120.

9. van Hall, T., A. Sijts, M. Camps, R. Offringa, C. Melief, P. M. Kloetzel, and F. Ossendorp. 2000. Differential influence on cytotoxic T lymphocyte epitope presentation by controlled expression of either proteasome immunosubunits or PA28. *J. Exp. Med.* 192: 483–494.
10. Yamano, T., S. Murata, N. Shimbara, N. Tanaka, T. Chiba, K. Tanaka, K. Yui, and H. Udono. 2002. Two distinct pathways mediated by PA28 and hsp90 in major histocompatibility complex class I antigen processing. *J. Exp. Med.* 196: 185–196.
11. Murata, S., H. Udono, N. Tanahashi, N. Hamada, K. Watanabe, K. Adachi, T. Yamano, K. Yui, N. Kobayashi, M. Kasahara, et al. 2001. Immunoproteasome assembly and antigen presentation in mice lacking both PA28α and PA28β. *EMBO J.* 20: 5898–5907.
12. Tanahashi, N., Y. Murakami, Y. Minami, N. Shimbara, K. B. Hendil, and K. Tanaka. 2000. Hybrid proteasomes: induction by interferon-γ and contribution to ATP-dependent proteolysis. *J. Biol. Chem.* 275: 14336–14345.
13. Baumeister, W., J. Walz, F. Zuhl, and E. Seemuller. 1998. The proteasome: paradigm of a self-compartmentalizing protease. *Cell* 92: 367–380.
14. Cascio, P., M. Call, B. M. Petre, T. Walz, and A. L. Goldberg. 2002. Properties of the hybrid form of the 26S proteasome containing both 19S and PA28 complexes. *EMBO J.* 21: 2636–2645.
15. Moore, M. W., F. R. Carbone, and M. J. Bevan. 1988. Introduction of soluble protein into the class I pathway of antigen processing and presentation. *Cell* 54: 777–785.
16. Udono, H., T. Yamano, Y. Kawabata, M. Ueda, and K. Yui. 2001. Generation of cytotoxic T lymphocytes by MHC class I ligands fused to heat shock cognate protein 70. *Int. Immunol.* 13: 1233–1242.
17. Porgador, A., J. W. Yewdell, Y. Deng, J. R. Bennink, and R. N. Germain. 1997. Localization, quantitation, and in situ detection of specific peptide-MHC class I complexes using a monoclonal antibody. *Immunity* 6: 715–726.
18. Bloom, M. B., D. Perry-Lalley, P. F. Robbins, Y. Li, M. el-Gamil, S. A. Rosenberg, and J. C. Yang. 1997. Identification of tyrosinase-related protein 2 as a tumor rejection antigen for the B16 melanoma. *J. Exp. Med.* 185: 453–459.
19. Uenaka, A., T. Ono, T. Akisawa, H. Wada, T. Yasuda, and E. Nakayama. 1994. Identification of a unique antigen peptide pRL1 on BALB/c RLδ1 leukemia recognized by cytotoxic T lymphocytes and its relation to the Akt oncogene. *J. Exp. Med.* 180: 1599–1607.
20. Glickman, M. H., D. M. Rubin, V. A. Fried, and D. Finley. 1998. The regulatory particle of the *Saccharomyces cerevisiae* proteasome. *Mol. Cell. Biol.* 18: 3149–3162.
21. Ma, C. P., P. J. Willy, C. A. Slaughter, and G. N. DeMartino. 1993. PA28, an activator of the 20 S proteasome, is inactivated by proteolytic modification at its carboxyl terminus. *J. Biol. Chem.* 268: 22514–22519.
22. Song, X., J. von Kampen, C. A. Slaughter, and G. N. DeMartino. 1997. Relative functions of the α and β subunits of the proteasome activator, PA28. *J. Biol. Chem.* 272: 27994–28000.
23. Weiss, W. R., S. Mellouk, R. A. Houghten, M. Sedegah, S. Kumar, M. F. Good, J. A. Berzofsky, L. H. Miller, and S. L. Hoffman. 1990. Cytotoxic T cells recognize a peptide from the circumsporozoite protein on malaria-infected hepatocytes. *J. Exp. Med.* 171: 763–773.
24. Aki, M., N. Shimbara, M. Takashina, K. Akiyama, S. Kagawa, T. Tamura, N. Tanahashi, T. Yoshimura, K. Tanaka, and A. Ichihara. 1994. Interferon-γ induces different subunit organizations and functional diversity of proteasomes. *J. Biochem.*115: 257–269.
25. Shimbara, N., K. Ogawa, Y. Hidaka, H. Nakajima, N. Yamasaki, S. Niwa, N. Tanahashi, and K. Tanaka. 1998. Contribution of proline residue for efficient production of MHC class I ligands by proteasomes. *J. Biol. Chem.* 273: 23062–23071.
26. Ustrell, V., L. Hoffman, G. Pratt, and M. Rechsteiner. 2002. PA200, a nuclear proteasome activator involved in DNA repair. *EMBO J.* 21: 3516–3525.
27. Ortega, J., J. B. Heymann, A. V. Kajava, V. Ustrell, M. Rechsteiner, and A. C. Steven. 2005. The axial channel of the 20S proteasome opens upon binding of the PA200 activator. *J. Mol. Biol.* 346: 1221–1227.
28. Morel, S., F. Levy, O. Burlet-Schiltz, F. Brasseur, M. Probst-Kepper, A. L. Peitrequin, B. Monsarrat, R. Van Velthoven, J. C. Cerottini, T. Boon, et al. 2000. Processing of some antigens by the standard proteasome but not by the immunoproteasome results in poor presentation by dendritic cells. *Immunity* 12: 107–117.
29. Rammensee, H. G., K. Falk, and O. Rotzschke. 1993. Peptides naturally presented by MHC class I molecules. *Annu. Rev. Immunol.* 11: 213–244.

Both CD4+ and CD8+ T cell epitopes fused to heat shock cognate protein 70 (hsc70) can function to eradicate tumors

Shusaku Mizukami,[1,2] Chiaki Kajiwara,[1] Hiroshi Ishikawa,[3] Ichiro Katayama,[3] Katsuyuki Yui[2] and Heiichiro Udono[1,4]

[1]Laboratory for Immunochaperones, Research Center for Allergy and Immunology (RCAI), RIKEN Yokohama Institute, 1-7-22 Suehiro-Cho, Tsurumi-Ku, Yokohama-Shi 230-0045; [2]Division of Immunology, Department of Molecular Microbiology and Immunology, Graduate School of Biomedical Sciences, Nagasaki University, 1-12-4 Sakamoto, Nagasaki 852-8523; [3]Department of Dermatology, Graduate School of Medicine, Nagasaki University

(Received October 15, 2007/Revised January 22, 2008/Accepted January 26, 2008/Online publication March 13, 2008)

Vaccination with heat shock proteins (HSP) protects mice from challenge with the tumor from which the HSP were isolated. The antigenicity of HSP vaccination is thought to result from HSP-associated endogenous major histocompatibility complex class I peptides or their precursors. The vaccination effect can be achieved in an adjuvant-free manner and is mediated by CD8+ T cells, indicating that HSP can act as a natural adjuvant and cross-prime T cells *in vivo*. We previously devised a recombinant vaccine composed of a CD8+ T cell epitope fused to the carboxyl-terminus of hsc70 and demonstrated efficient generation of antigen-specific cytotoxic T lymphocyte (CTL) after vaccination with a few micrograms of the hsc70-CTL epitope fusion protein. The present study aimed to determine if the fusion protein vaccine could control tumor growth *in vivo* and whether simultaneous fusion of a CD4+ T cell epitope to the amino terminus of the hsc70-CTL epitope would be a more potent vaccine compared to the CTL epitope alone. Ovalbumin (OVA)-derived 8 mer peptide, $OVA_{257-264}$, and 16mer peptide, $OVA_{265-280}$, were used as CD8+ and CD4+ T cell epitopes, respectively. Vaccination with hsc70-$OVA_{257-264}$ generated peptide specific CTL more effectively than a peptide plus incomplete Freund's adjuvant combination, and suppressed growth of OVA expressing EL4 (E.G7) and B16 melanoma tumor cells. Addition of $OVA_{265-280}$ to the amino-terminus of hsc70-$OVA_{257-264}$ ($OVA_{265-280}$-hsc70-$OVA_{257-264}$) enhanced the generation of the $OVA_{257-264}$-specific CTL population, leading to better eradication of MO5 lung metastasis compared to hsc70-$OVA_{257-264}$. Our results suggest that fusion of both CD4+ and CD8+ T cell epitopes to hsc70 enhances tumor immunity beyond the effect of the CD8+ T cell epitope alone. (*Cancer Sci* 2008; 99: 1008–1015)

Heat shock proteins (HSP) have been implicated as tumor rejection antigens *in vivo*, for example vaccination with HSP gp96, hsp90, and hsc70, even without adjuvants, protects mice from challenge by the tumors from which the HSP were originally isolated.[1–3] The immunogenicity of HSP vaccines has been suggested to result from carry-over of endogenous peptides that were associated with HSP in cells, and not due to HSP *per se*.[1] Indeed, we previously identified major histocompatibility complex (MHC) class I ligands or their precursors that were acid-eluted from gp96, hsp90, and hsc70 derived from the radiation leukemia, RL♂1.[4] An important observation from those studies was that the quantity of tumor antigen peptides associated with HSP was no more abundant than we expected. Thus, it was surprising that such a tiny amount of peptide was sufficient to prime CD8+ T cells that enabled tumor rejection *in vivo*. These findings raise the fascinating possibility that HSP may serve as potent and safe natural adjuvants, better than any now available.

The recent observation that toll-like receptors (TLR) 4 and 2 interact with gp96 or hsp70, resulting in production of pro-inflammatory cytokines by antigen presenting cells (APC)[5,6] may provide the rationale behind the strong HSP adjuvant effect, since activation of APC is essential for the full-priming of T cells. In addition, HSP seemed to target a number of receptors such as CD91,[7] LOX-1,[8] and SRA[9] on dendritic cells (DC) or macrophages *in vivo*. HSP are efficiently captured by these receptors on DC and internalized into endosome/lysosome compartments in which peptides associated with HSP are channeled into the cytosol, probably through a retro-translocation mechanism via a translocon consisting of Sec61 and p97.[10] The peptides released into the cytosol are on a track to a classical MHC class I antigen-processing pathway to be presented to CD8+ T cells. This conceptual mechanism for HSP-induced immunity encouraged us to construct a novel recombinant vaccine in which MHC class I ligands are covalently fused to either the carboxyl- or amino-terminus of hsc70. In these fusion proteins, each hsc70 molecule contained at least one T cell epitope, thus the number of specific peptides associated with HSP was dramatically increased, in comparison with the natural HSP purified from tumor cells. Moreover, presentation of HSP-bound self-peptides that might evoke autoimmunity could in principle be avoided. We previously showed that specific CTL were easily generated against five distinct CD8+ T cell epitopes by vaccination with a few micrograms of those hsc70-peptide complexes,[11] but the protective efficacy of this approach against *in vivo* tumor growth has not been investigated. Another issue to be addressed is how CD4+ T cells modulate HSP-mediated immunity. HSP-induced cross-priming of CD8+ T cell does not require CD4+ T cells.[11,12] Nonetheless, it is also true that antigen-specific CD4+ T cells are activated by vaccination with antigen-HSP complexes.[13]

In the present study, we investigated whether vaccination with CTL epitopes fused to hsc70 could protect against tumor growth *in vivo*. We also examined whether simultaneous fusion of a helper epitope in addition to CTL epitope to hsc70 gives rise to the enhanced protection over the effect of CTL epitope alone.

Materials and methods

Cell lines. EL-4 is a methylchoranthlene-induced thymoma of C57BL/6(H-2^b) origin. E.G7 is an OVA cDNA transfected EL-4 cell line. B16 is a melanoma cell line derived from C57BL/6, and MO5 is an OVA cDNA transfected B16 cell line.

Media and cell cultures. RPMI-1640 was supplemented with nonessential amino acids (Gibco/BRL, Tokyo, Japan), glutamine, sodium pyruvate, antibiotics (all from Sigma, St Louis, MO, USA), 10% fetal calf serum, and 5×10^{-5} M 2-Mercaptoethanol. This complete RPMI media was used for CTL induction and tumor cell culturing. E.G7 was cultured in the presence of 500 μg/mL G418.

*To whom correspondence should be addressed. E-mail: udonoh@rcai.riken.jp

doi: 10.1111/j.1349-7006.2008.00788.x